Investigating the Role of Lipid Droplets in Stress Response Regulation in *S. cerevisiae*

Jack Davis

Cell Biology Msc

School of Biosciences

University of Kent

Supervisor: Dr Campbell Gourlay

Declaration

No part of this thesis has been submitted in support of an application for any degree or qualification of the University of Kent or any other university or institute of learning.

Jack Davis

Acknowledgements

I would first like to thank Dr Campbell Gourlay, without whom I would not be undertaking this project. He gave me the opportunity to begin, what I hope, to be a long and fruitful career in research.

Secondly, to Dr Patrick Rockenfeller, whose guidance and teachings proved invaluable and to whom I owe my increasing passion for science.

I owe a lot to everybody within the Gourlay lab, particularly Elliot Piper-Brown, who was always there to lend a helping hand and discuss any and all issues throughout the year.

Finally, the support from my parents and to my partner, Rafaella, inspired me to give my all to this first stage of my career. These works are dedicated to them.

Table of Contents

Abbreviations

µm- Micrometre

µM- Micromolar

µL- Microlitre

AMP- Ampicillin

are1p- . Acyl-Coenzyme A: sterol acyltransferase 1

are2p-. Acyl-Coenzyme A: sterol acyltransferase 2

ayr1p- 1-Acyldihydroxyacetone-phosphate reductase

Bp- Basepair

cho2p- Phosphatidylethanolamine N-Methyltransferase

CTP- Cytidine Triphosphate

CCT- CTP:phosphocholine cytidyltransferase

CWI- Cell wall integrity

DAG- Diacylglycerol

DAGAT- acylcoenzyme A: Diacylglyceride acyltransferases

dga1p- Acyl Coenzyme A: Diacylglyceride acyltransferase 1

dGAT1- Diacylglycerol Acyltransferase 1

DNA- Deoxyribonucleic Acid

E.coli- Escherichia coli

EM- Electron microscopy

EMC- Endoplasmic Reticulum Membrane Protein Complex

ER- Endoplasmic Reticulum

ERMES- Endoplasmic Reticulum- mitochondria engagement structure

FA-fatty acid

fld1p- Few Lipid Droplets 1

Gem1- GTPase EF-hand protein of Mitochondria

gat1p- Glycerol-3-phosphate acyltransferase 1

GEF- Guanine exchange factor

GPI- glycosylphosphatidylinositol

GTP- Guanosine triphosphate

IMM- Inner mitochondrial membrane

IMS- Intermembrane space

ino2p- Inositol Requiring 2

ino4p- Inositol Requiring 4

Kb- Kilobase pair

LD- Lipid Droplet

ldb16- Low dye binding 16

lro1p- Lecithin cholesterol acyl transferase related open reading frame

loa1- Lysophosphatidic acid acyltransferase 1

ltc1- lipid transfer at contact site 1

MAPK- Mitogen activated protein kinase

Mdm- Mitochondrial distribution and morphology protein

Mmm1- Maintenance of Mitochondrial Morphology 1

PA- Phosphatidic Acid

Pah1p- Phosphatidate Phosphatase

PC- Phosphatidylcholine

PCR- Polymerase Chain Reaction

PE- Phosphatidylethanolamine

PEMT- Phosphatidylethanolamine N-Methyltransferase

PI- Phosphatidylinositol

pkc1- Protein kinase C

PIP_2- Phosphattodylinositol 4,5-bisphosphate

PS- Phosphatidylserine

Psd1- Phosphatidylserine Decarboxylase 1

rho1- Ras homolog 1

rom2- Rho multicopy suppressor

Rpm- Rotations Per Minute

S. Cerevisiae- Saccharomyces Cerevisiae

SD- SD- Yeast Selective Dropout

SE- Sterol Ester

SLD- Supersized Lipid droplet

ssDNA- Single Stranded Carrier DNA

TAG-Triacylglyceride

TE- Tris- EDTA

TGL- Triacylglycerol Lipase

TM- Transmembrane

Tus1- TOR unique function suppressor

VLCFA- Very Long Chain Fatty Acid

WT- Wild Type

YPD- Yeast Extract, Peptone, Dextrose

YNB- Yeast Nitrogen Base

Abstract

Lipid droplets are spherical lipid storage vesicles that sequester fatty acids as the “neutral lipids” in a manner that is non-toxic to the cell. Creation of the primary neutral lipid within a lipid droplet’s core, triacylglycerol (TAG) is controlled by Dga1 and Lro1, with sterol ester (SE) formation being controlled by Are1 and Are2. This work reveals that disruption of the actin cytoskeleton, or exposure to a variety of stresses that trigger cell wall integrity (CWI) signalling, promotes formation of lipid droplets. We propose that formation of lipid droplets is an important step within CWI signalling, as deletion of *DGA1* and *LRO1*, a disruption of TAG synthesis, prevent pathway activation. I show that constitutive activation of CWI signalling leads to a lipid droplet dependent increase in necrosis, suggesting a mechanism by which cells that cannot adapt to stress may be removed from the population. Unpublished work from our lab has established the presence of the mitochondrial outer membrane protein, porin, as a necessary component of the CWI pathway. This data outlines a novel mechanism through which mitochondria and lipid droplets facilitate CWI signalling and cell fate decisions in yeast.

Chapter 1

Introduction

1.1 Lipid droplet regulation and interactions in *Saccharomyces cerevisiae*

1.1.1- Lipid Droplet Morphology

Lipid droplets (LD) have been well established as a means for eukaryotes to store excess fatty acids in a neutral and non-toxic manner[1,2] composition varies depending on the eukaryote, but the general structure is the same; a hydrophobic neutral lipid core, surrounded by a phospholipid monolayer[2,3,12–14,4–11]. Two types of neutral lipids make up the core: triacylglycerides (TAG), and steryl esters (SE). TAG molecules consist of a glycerol backbone, with three fatty acid (FA) groups attached by ester bonds[12], whereas SEs are comprised of a sterol group esterified with a FA molecule[15]. The structure of a lipid droplet can be seen in figure 1.1.1

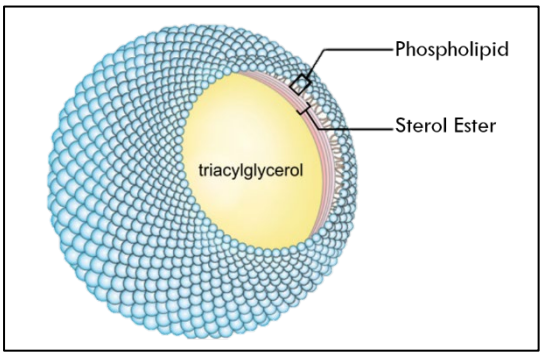

Figure 1.1.1 Structure of a lipid droplet A lipid droplet comprises a core of TAG and SE, encapsulated by a phospholipid monolayer along with associated proteins. Image adapted from Wang *et al 2015*

In the yeast *Saccharomyces cerevisiae (S. cerevisiae)*, the average LD neutral core is composed of both TAG and SE in equal measure [1], with TAG forming the centre of the LD, surrounded by multiple layers, or "shells", of SE [16]. The phospholipid monolayer of LDs in *S. cerevisiae* is predominantly phosphatidylcholine (PC) (which plays a significant role in LD size regulation),

phosphatidylinositol (PI) and phosphatidylethanolamine (PE) [1], but with notable concentrations of glycerophospholipids such as lyso-PC and lyso-PE[17]. The general size for a LD in *S. cerevisiae* is approximately 0.3-0.4 micrometres (µm) in diameter[6], although this varies greatly in certain mutants that'll be discussed later in this chapter.

1.1.2 Lipid Droplet Formation

LDs and their biogenesis is strongly linked to the endoplasmic reticulum (ER)[10,18–20].The most popular model for LD biogenesis is the accumulation of neutral lipids within the phospholipid bilayer of the ER, gradual curvature of the membrane[6,10,21,22], the formation of a "lens", and the eventual budding of the LD from the ER [1,6,8,18,21] (Figure 1.1.2a)

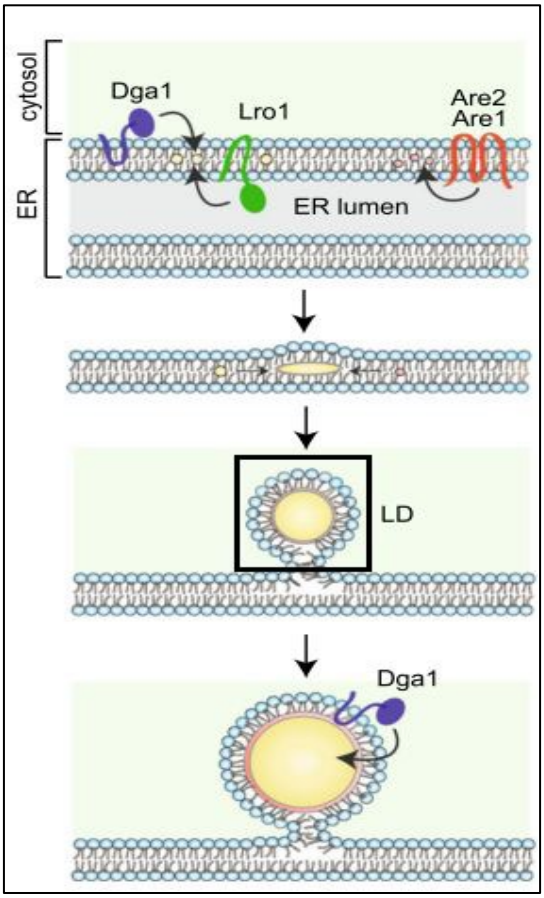

Figure 1.1.2a Formation of a lipid droplet

The proposed model of lipid droplet formation, displaying accumulation of neutral lipids within the ER bilayer and budding from the ER. Image adapted from Wang *et al 2015*

The synthesis of neutral lipids, and therefore of LDs, is known to be controlled by four ER associated enzymes. Acyl coenzyme A: diacyl-glycerol acyltransferase 1 (Dga1p), encoded by the *DGA1* gene[2,3,28,8,16,18,23–27], and Lecithin cholesterol acyl transferase related open reading frame (Lro1p) encoded by *LRO1*[3,8,16,18,23,25–29], are solely responsible for TAG production. Acyl-Coenzyme A: sterol acyltransferases 1 and 2 (Are1p and Are2p), encoded by the genes *ARE1* and *ARE2* respectively, mediate the formation and accumulation of SEs within newly forming LDs[16,23,25–28].

TAG synthesis through the action of Lro1p requires the TAG precursor diacylglycerol (DAG) and a phospholipid donor, specifically PC. The enzyme Lro1p catalyses the transfer of a FA from PC and subsequent esterification of DAG to form TAG[8,16,18,23,26–28]. Topological analysis of Lro1p showed it to be a transmembrane protein with a catalytic domain that lays within the ER lumen, suggesting this particular reaction takes place there[18], which is a stark contrast to Dga1p which has its catalytic domain within the cytosol[18]. Dga1p, a member of the acyl-coenzyme A diacylglycerol acyltransferase (DAGAT) family, utilises acyl-CoA molecules as a FA source for DAG esterification[2,3,15,18,25,30,31]. *dga1Δlro1Δ* mutants lacking activity of each enzyme reveal an almost complete loss of TAG sequestration[8,12,25,27], displaying the near exclusivity of TAG biosynthetic activity to the two enzymes. Further knockout of Are2p, known to elicit TAG synthetic activity to a small degree, displays a phenotype with a complete lack of TAG[25].

The synthesis of SE neutral lipids within the ER leaflet is undertaken by enzymes Are1p and Are2p through very similar activities- ergosterol is a viable substrate for both[16,23,26–28],

whereas Are1p, which in *S. cerevisiae* is upregulated during periods of anaerobic respiration and starvation, uses ergosterol and its' precursors to form sterol esters[23]. Much like TAG synthesis by Dga1p, Are1p and Are2p use Acyl-CoA as a FA donor[16,23,27,28].

Using quadruple knockout mutants as a model (*dga1Δlro1Δare1Δare2Δ*), it has been shown that TAG synthesis is more important for the formation of LDs than SE. The quadruple mutant displays a phenotype with no LD proliferation[25,27]. Transformation of *DGA1* and *LRO1* containing plasmids into this mutants saved the LD phenotype, whereas transforming with an *ARE2* containing plasmid resulted in no LD formation[27].

A fifth enzyme shown to be of great importance for LD biogenesis is phosphatidate phosphatase (Pah1p), encoded by the *PAH1* gene[2,9,10,32–36]. While Pah1p is not directly responsible for neutral lipid synthesis, *pah1Δ* mutants display a significantly lower TAG content than the wild type (WT)[10,36], a resultant increased SE composition of LDs[36] and an approximately 65% drop in LD formation[10]. A *pah1Δare1Δare2Δ* triple mutant (devoid of SE biosynthetic pathways) shows a phenotype completely lacking in LDs, unless subjected to very high oleic acid concentrations. Pah1p affects TAG synthesis as it is responsible for the production of its precursor, DAG, from phosphatidic acid (PA)- a conversion that makes it a key regulatory enzyme in maintaining the phospholipid/ neutral lipid homeostatic balance[9].

Pah1p activity is regulated by the transmembrane (TM) phosphatase complex, Nem1p-Spo7p [10,36], and by the Cdc28p (Cdk1) protein kinase[10]. In its phosphorylated form following the

action of Cdk1, Pah1p is unable to synthesise DAG from PA- PA levels rise, DAG levels fall and TAG synthesis is hindered as a result[2,10,32–36]. The Nem1p-Spo7p holoenzyme, however, is responsible for dephosphorylation of Pah1p, and therefore a derepression of DAG synthesis [10,32,36], providing ample DAG for Dga1p and Lro1p to synthesise TAG (Figure 1.2.1b).

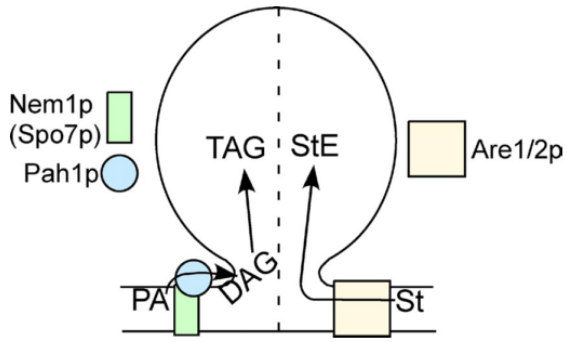

Figure 1.2.1b Nem1p-Spo7p complex facilitates DAG synthesis The conversion of PA to DAG relies on Pah1, whose activity is regulated by the Nem1-Spo7p holoenzyme. Image sourced from *Adeyo et al, 2011*[10]

As previously mentioned, the gradual sequestration of neutral lipids within the leaflet of the ER bilayer is coupled with a curvature of the membrane[10,21,22,37], but the mechanism for this isn't understood particularly well. It has been noted that the phospholipid composition of regions surrounding lens formation do not wholly match the composition of the rest of the ER bilayer, and some go as far as to suggest that phospholipid "demixing", or the process by which membrane composition is locally altered, is the cause of membrane curvature during lens formation[21]. The phospholipid PA, and lysophospholipid lysophosphatidic acid (LPA)[22] are thought to be involved in curving the membrane, due to a negative and a positive "cone shape"[22,37] respectively. It is also suggested that higher concentrations of DAG within the membrane have an impact on its curvature due to instability, a small head group (when compared to that of PA) and the ease with which it can flip-flop within a bilayer.[10]

1.1.3 Lipid Droplet Growth

Following their budding from the ER, LDs may grow depending on the needs of the cell (for example, during periods of high oleic acid concentration so as to sequester toxic FAs[28,38–40]). The general mechanism for this would be further TAG synthesis, which can take place directly on LDs as Dga1p may remain localized to LD monolayer following LD biogenesis[2,3,8]. To accommodate the additional TAG, further PC synthesis takes place, following a phospholipid synthetic pathway called the "Kennedy Pathway"[2,6,7,32,36,41,42]. The Kennedy pathway is responsible for the production of both PC and PE from their precursors (choline and ethanolamine, respectively) by phosphorylation, association with cytidine triphosphate (CTP) and subsequent transfer of the phosphoaminoalcohol group to DAG[41–43] (Figure 1.1.3). The rate limiting step of PC formation in the Kennedy pathway is the association with CTP, which is catalysed by the enzyme CTP:phosphocholine cytidyltransferase (CCT)[41–43], an enzyme that localises to LDs[41]. It should be noted that the Kennedy pathway is not the primary mechanism for PC synthesis (the absence of choline within the cell still results in sufficient PC synthesis[41,42]), as there is another pathway called the phosphatidylethanolamine N-methyltransferase pathway, or PEMT pathway[2,6,19,42]). The PEMT pathway methylates PE in three stages through the action of PEMT enzymes, Cho2p and Opi3p[6,19,41,44].

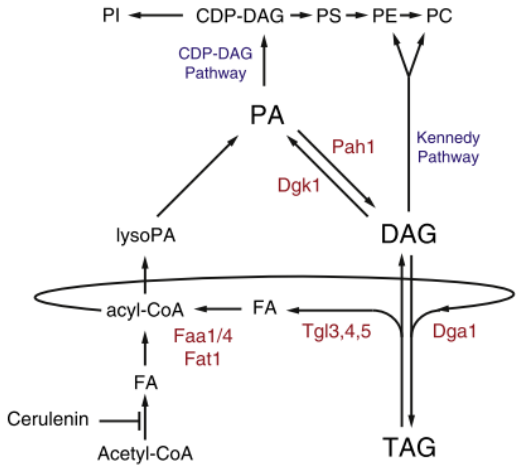

Figure 1.1.3 Kennedy and CDP-DAG Pathways An outline of lipid metabolism surrounding lipid droplet growth and mobilisation of TAG from lipid droplets. TAG may be readily converted to FFAs and DAG for phospholipid synthesis[2]. Image sourced from *Markgraf et al, 2014*[2]

It is well documented that under certain circumstances, LD size may deviate greatly from the norm[4,11,19,37,45]. Some mutants display a phenotype with supersized lipid droplets (SLDs)[4,6,19], growing up to 50 times larger in volume than in the wild type[37]. A gene deletion study completed by Fei et al revealed an array of genes that seem to be key in the regulation of LD size, the knockout of which leads to a formation of these SLDs[37]. The most prominent group of genes revealed were those with a direct or indirect link to phospholipid synthesis, including: *INO2* and *INO4*, which both act as phospholipid biosynthetic pathway promoter genes encoding transcription factors Inositol Requiring 2 and 4 (ino2p and ino4p respectively)[37,46–50]; *CHO2* and *OPI3*, both encoding PEMTs (Cho2p and Opi3p), responsible for catalysing methylation of PE in the PEMT pathway[19,37]; and *CDS1*, encoding CDP-Diacylglyerol synthase 1[37]. The genes listed previously are all in some form or another linked with phospholipid synthesis, predominantly PC through the Kennedy or PEMT pathways[19,37,46–50]. It stands to reason, then, that because mutants such as *cho2Δ*, *opi3Δ*,

ino2Δ and *ino4Δ* display an SLD phenotype, the synthesis of phospholipids is particularly important for the regulation of LD size.

FLD1, a gene which encodes for a seipin homologue, few lipid droplets 1 (fld1p)[4,19,36,37], was also flagged up as key gene for the regulation of LD size- the deletion of this gene yielded a SLD phenotype with very few lipid droplets[4,6,19,51]. This protein has a propensity to localize to ER-LD contact sites[4,6,19,51]. fld1p, however, is not associated with the biosynthesis of phospholipids like the other genes in the study, but instead is believed to be a regulator of LD dynamics due to an increased propensity for aggregation of LDs in an *fld1Δ* mutant- the LD population displayed by this particular mutant has a split morphology, displaying either minimal SLDs, a large number of very small LDs, or a large cluster of regular sized LDs[4,6,51]. With this *fld1Δ* mutant, a fusion of LDs was observed at these sites of aggregation[4,6,19], as well as purified LDs from the same mutant[4]; a mechanism that would explain the presence of SLDs in this particular genotype. The *fld1Δ* mutant also displays higher quantities of medium to short chain fatty acids within the cells' phospholipids compared to a higher long chain composition in the wild type[4], coupled with elevated PA incorporation into LDs and other phospholipid membranes[19,51]; a characteristic shared with *cho2Δ*, *opi3Δ*, *ino2Δ* and *ino4Δ* [4,6,51].

An additional protein, Low Dye Binding 16 (Ldb16p), causes the same phenotype when deleted[4,19,51,52]. Ldb16 is a TM protein of the ER that localises to ER-LD contact sites, and has implications in the maintenance of regular sized LDs[19,51]. Both ldb16p and fld1p were shown to interact with one another through means of a yeast two-hybrid assay and a tandem affinity

purification, and in the *fld1Δ* mutant, ldb16p levels are much lower, suggesting an interaction between the two proteins and a potential stabilising role for fld1p; this loss of ldb16p could be rescued with the addition of MG132, a proteasome inhibitor[19]; an observation that suggests that under normal circumstances, ldb16p is subject to endoplasmic reticulum associated degradation (ERAD) when not in the presence of fld1p[19,51].

It has been speculated that the collaboration between fld1p and ldb16p is important for LD size regulation at ER-LD contact sites[19,51]. Negative staining electron microscopy (EM) displayed fld1p forming a ring-shaped homo-oligomeric structure with 9 copies of itself[19,51], but neither the fld1p monomers nor the oligomer form a region with enzymatic activity[19], suggesting a more of a facilitative role at the ER-LD contact site. Because the same phenotype arises in both *lbd16Δ* and *fld1Δ*, and ldb16p displays a reliance on the presence of fld1p, it is apparent that the two co-operate; Grippa *et al* suggest the presence of an fld1p-lbd16 complex at ER-LD contact sites helps to stabilise the site, and facilitate the regulated diffusion of phospholipids from the ER to LDs[51], a process by which LD growth can be controlled.

1.1.4 Lipid Droplet Breakdown

The breakdown of LDs, first and foremost, is a method by which the cell is able to utilize sequestered free FAs- be it for energy or for lipid metabolism[5,53–56]. These FAs are locked within the neutral lipid core of LDs, predominantly in the form of TAG. The breakdown of TAG is mainly orchestrated by enzymes dubbed Triacylglycerol lipases (TGL).

The first TGL to be discovered was Tgl3p, encoded by the Gene TGL3[54,57,58]. Structural analysis of the enzyme's secondary structure displays a highly hydrophobic C-terminus, coupled with a complete lack of TM spanning domains[57,59]; this is typical of LD associated proteins, due to the presence of a hydrophobic core and only a monolayer in which to embed as opposed to a bilayer[2,6,53,54,57,59–61,7–14]. In Tgl3p mutants with a truncated C-terminus, there is notable TAG accumulation due to instability and loss of function, stressing the importance of the lipases' hydrophobic region[59]. Tgl3p is found exclusively associated with LDs- western blot analysis of *S. cerevisiae* expressing Tgl3p-GFP displayed tagged Tgl3p in no fraction other than the LD fraction[57]. A *tgl3Δ* mutant displays sporulation defects, has increased TAG content, but TAG mobilization (the release of TAG FAs from LDs) isn't completely abolished; this is due to the presence of other TGLs[54,57]. Tgl4p and Tgl5, both homologues of Tgl3p, display the same degree of LD association, coupled with similar characteristic structures; hydrophobic C-termini and lack of TM regions[54,62]. They contribute less to the overall TAG mobilization due to exhibiting specificities: Tgl5p predominantly catalyses the mobilization of very long chain fatty acids (VLCFAs), Tgl4p displays a preference for myristic acid and palmitic acid chains, whereas Tgl3p has a much broader range of substrates[58,63]. Interestingly, an additional TGL exists within mitochondria: Tgl2p[64], although there is very little literature regarding the true purpose of this protein. Tgl4p, alongside TAG lipase activity, has also been implicated in the hydrolysis of SEs, lysophospholipid acyltransferase activity (acylation of LPA to yield PA), and even regulation of phospholipid composition, with the *tgl4Δ* mutant displaying altered PA and PC levels[62].

Schmidt, and subsequently Klein, using mutants defective in TAG synthesis, SE synthesis and LD biogenesis (*Dga1ΔLro1Δ*, *Are1ΔAre2Δ* and *Dga1ΔLro1ΔAre1ΔAre2Δ* respectively) aimed to characterise the regulation of TGLs[58,63]. A mutant devoid of LDs displayed a very similar level of *TGL3* gene expression when compared to the WT[58], an observation which is much the same for *TGL4* and *TGL5*[63]. Despite this, Tgl3p level were approximately 50% of that of the WT[58], but the same cannot be said for Tgl4p and Tgl5p; both of these appeared in very similar quantities across all mutants, and were merely relocated to the ER, maintaining catalytic activity as lysophospholipid acyltransferases[62,63]. The significant drop in Tgl3p is notable in all mutants with TAG synthesis defects, which may suggest an effect of TAG absence on the stability of this particular TGL. Additional works to attempt to establish a link between the regulation of the three TGLs using *tgl4Δtgl5Δ*, *tgl3Δtgl5Δ tgl3Δtgl4Δ* mutants revealed that there was no major discernible change in expression of each gene as a result of deletions of the other. This, coupled with the differences in response to lack of LDs, suggests that the three TGLs, whilst fulfilling a similar role in TAG mobilization, are fairly distinct from one another[62,63].

Initially, a TGL triple mutant (*Tgl3ΔTgl4ΔTgl5Δ*) displayed a complete lack of TAG mobilization, coupled with an inability to sporulate[54]. However, more recent works with this particular TGL triple knockout showed that, when cultured on a plate with excess oleic acid, aside from oversized LDs and an abundance of peroxisomes (excessive neutral lipid synthesis required to avoid oleic acid toxicity) there's still an element of TAG lipolysis, suggesting the presence of further TAG hydrolytic enzymes[61], although as of yet it is unclear as to why TAG lipolysis would be occurring in this mutant in an excess of FAs.

1-Acyldihydroxyacetone-phosphate reductase (Ayr1p) has since been implicated as one of the major enzymes involved in mobilization of TAG from LDs[61,65]; overexpressing the *AYR1* gene causes a notable reduction in intracellular TAG, and in vitro, Ayr1p displayed it was capable of exhibiting lipase activity at a markedly higher efficiency than that of a known lipase, Lpx1p[61]. That having been said, it's still believed that other, more hydrolytic enzymes aid in TAG mobilization, as there is still a small hydrolytic activity in the absence of Tgl3p, Tgl4p, Tgl5p and Ayr1p[61]. Notably, Ayr1p also contributes to PA synthesis; it's been suggested that this enzyme works in tandem with Tgl3p, receiving freed FAs as substrates for PA synthesis[56].

SE hydrolysis is slightly less useful as an energy source than TAG breakdown due to the presence of only one associated FA as opposed to three[12,15], but SE mobilization produces sterol, the precursor necessary for ergosterol production in the ER[15,27,66–69]. The hydrolysis of SE is controlled by three known enzymes: Yeh1p[54,68,69], Yeh2p[54,68–70] and Tgl1p[54,68,69].

1.1.5 Roles of Lipid Droplets Within the Cell

As has been touched upon in this review, one of the primary and best-established functions of LDs is the sequestration of excess FAs as TAG and SE within a neutral lipid core[2,3,14,71,5,7–13]. When cells contain an excess of free FAs, they begin to succumb to the effects of lipotoxicity; these lipid species may exude cytotoxic effects including mitochondrial dysfunction[72], difficulty in organellar membrane formation, a general loss of cell integrity[28,38,40,72,73], and eventual triggering of cell death pathways[35,38,40,74,75]. These effects are very readily apparent

in that of a total LD knockout mutant[28], and LDs in WT can be seen in greater numbers or even appear larger under these conditions[7,76],displaying their capacity to efficiently sequester these FA species.

LDs are a very useful source of energy; as required, when *S. cerevisiae* has exhausted any other available fermentable carbon source such as sugars, the lipolysis of neutral lipids within LDs provides a steady supply of substrate for β-oxidation[55,75,77,78]. They are also targets of microautophagy during stationary phase[79,80], at times of nitrogen starvation, or following disruption of fatty acid synthesis[80].

The sequestration of lipid molecules as neutral lipids also gives rise to a source of phospholipid precursors, should the need arise. Lipolysis of TAG yields DAG, a common precursor for phospholipids such as PC[41]. The dynamic ability of LDs to sequester and mobilize their contents to satiate the needs of the cell are what make them important.

1.1.6 Lipid Droplet Biogenesis Under Stress

As previously mentioned, LDs may form and grow when cells are exposed to higher levels of free FAs[7,52]. In *S. cerevisiae*, a visible increase in LDs can be seen when exposed to an excess of Oleic acid[7]; a means of preventing lipotoxicity. In a *gat1Δ* mutant (one devoid of Gat1p, or glycerol-3-phosphate acyltransferase 1), where one of the TAG precursor biosynthetic pathways is knocked out, there are no additional LDs formed following administration of excessive oleic acid, and indeed these cells became sensitive to oleic acid and colonies

struggled to proliferate in its presence[7]. The same phenotype can be seen in *loa1Δ* mutants; the Loa1 protein is a lysophosphatidic acid acyltransferase that catalyses a conversion in the same TAG synthetic pathway as Gat1p[9], which shows how important the formation of TAG is for combating cell lipotoxicity within yeast.

Excess LD biogenesis has been noted during times of starvation, particularly when cellular organelles are undergoing autophagy[72,81,82]. Orchestrated by the ER bound protein DGAT1 (diacylglycerol acyltransferase 1)[72,83], excess of FAs yielded through organellar breakdown during periods of autophagy are directed toward the ER membrane for LD biogenesis[72]. LDs can be located in abundant clusters near mitochondria during this period. DGAT1 knockouts led to a reduced formation of LDs during starvation induced autophagy[72], and it has also been noted that this mutation impedes cell viability; an increased concentration of acylcarnitine seems a possible candidate, as they exhibit potential lipotoxic effects towards mitochondria[72].

1.1.7 Cell wall Integrity Signalling

While indirect, LDs may play a role in the restructuring and synthesis of the fungal cell wall[84,85]; the ability for LDs to store TAG allows for the release of much needed DAG as the cell requires, and DAG is a much needed component in the formation of glycosylphosphatidylinositol-modified (GPI) proteins[86–88]. Previous works undertaken by the Gourlay lab (unpublished) have also suggested a larger role for lipid droplets in the cell wall integrity (CWI) pathway, which will be briefly outlined.

CWI is a branch of the mitogen-activated protein kinase (MAPK) signalling pathways that is highly conserved in fungal eukaryotes. CWI is concerned with cell wall remodelling and maintaining general morphology of the cell, ensuring correct progression throughout the cell cycle[89], as well as translating exogenous stresses upon the cell, such as osmotic[84,90–92] or heat shock[93,94] into an intracellular response that reacts accordingly.

CWI signalling is coordinated by Ras homolog (Rho1), a GTPase[95–98]. Rho1p may be activated in one of two ways: activation by its guanine exchange factors (GEF), Rho1 multicopy suppressor (Rom2)[94,95,98] and TOR Unique function suppressor (Tus1)[89,99,100], as a result of cell cycle progression, or activation by Rom1/2 due to a perceived cell wall stress detected by mechanosensors Wsc1-3[95,96,101] and Mid2[95,102].

Wsc1p and Mid2p sit within the plasma membrane and have been attributed to sensing cell wall stress in the wake of a variety of stresses that assert a stretch upon the cell wall. Upon sensing this stress, recruitment of Rom2p to the plasma membrane is orchestrated by phosphatidylinositol 4,5 bisphosphate (PIP_2)[103,104] (Figure 1.1.7a) Here, Rom2p may associate with Wsc1p and fulfil its role as a Rho-GEF, eliciting nucleotide exchange on the inactive Rho1p and activating it.

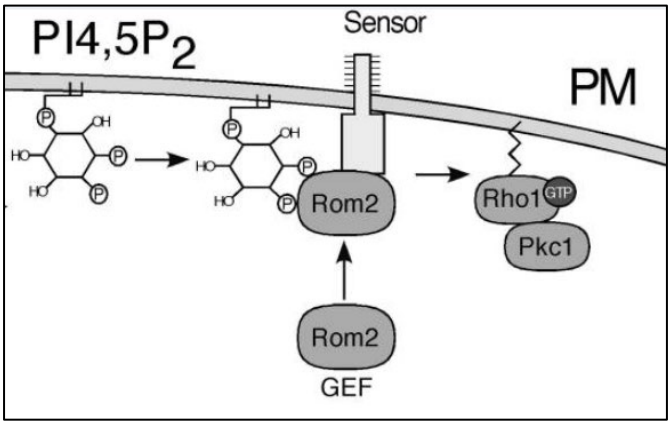

Figure 1.1.7a Activation of Rho1 by Rom2 The recruitment of to Wsc1 by PIP_2 facilitates the activation of Rho1 by nucleotide exchange, allowing for activation of Pkc1[103]. Image sourced from *Levin, 2005*[91]

Activation of Rho1p allows for induction of CWI signalling through the effector, protein kinase C (Pkc1)[95,98,101,105], which also requires the presence of cofactor PS[106]. Activation of Pkc1p initiates the CWI signalling cascade (Figure 1.1.7b) that terminates at the MAPK, Suppressor of the LyTic phenotype (Slt2)[101,102,107,108]. Following phosphorylation, Slt2p implements a negative feedback loop on the cascade by causing Rho1p to delocalise from the plasma membrane[102] to discourage overactivation and excessive cell wall generation. The MAPK also activates transcription factors such as Rlm1 and Swi4[109,110], both of which contribute to upregulating the gene expression of *FKS2*[101,109], a gene which encodes for β1,3- glucan synthase (GS)[85,105,107,111]. Upregulation of glycogen synthase in response to cell wall stress allows for restructuring of the cell wall through synthesis of of β1,3-glucan[85,105,112]. The potential link between lipid droplets and the CWI signalling pathway will be explored further throughout this study.

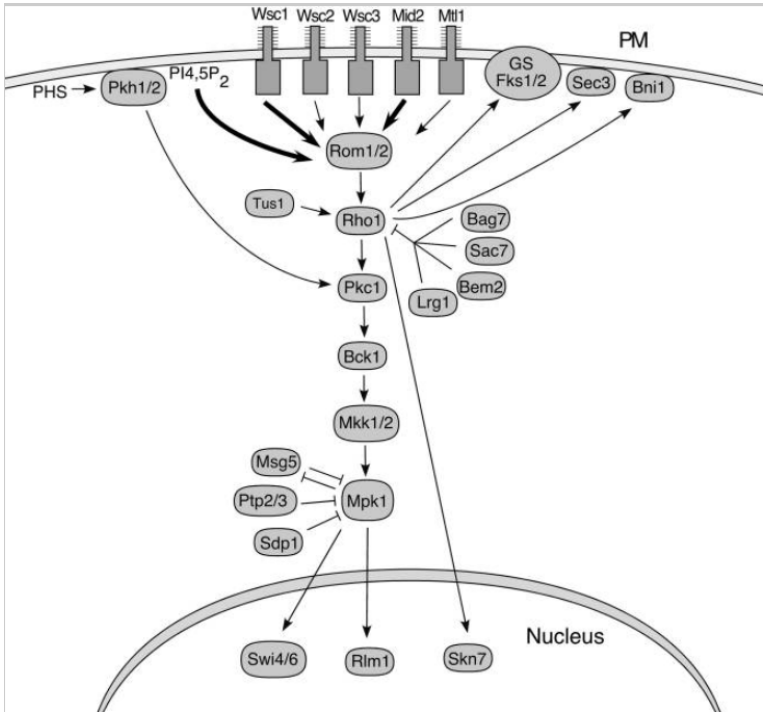

Figure 1.1.7b An overview of CWI signalling Activation of Rho1 by its GEFs following cell wall stress initiates a signalling cascade that promotes cell wall synthesis and remodelling in the face of stress and growth resumption[93,112]. Image sourced from *Levin, 2005*[91]

1.2 The Role of Mitochondria in Lipid Biogenesis

1.2.1 Mitochondria- Endoplasmic Reticulum Contact Sites

Membrane bound organelles may interact with one another for many reasons: extensive research exists into the interaction between the mitochondria and ER. This interaction is dubbed an "endoplasmic reticulum-mitochondria contact site"[43,113,122–126,114–121], and has been implicated in a number of roles important for cell viability and survival, including phospholipid transfer and mitochondrial membrane biogenesis[114–116,118,119,121–123,126,127], mitochondrial division[44,117] and mitophagy of dysfunctional and damaged mitochondria.[120,121].

At the heart of the ER-mitochondria contact site is the Endoplasmic Reticulum Mitochondria Encounter Structure (ERMES)[114,117,118,120,121,126,128], a protein complex formed between Mitochondrial distribution and morphology proteins 10, 34 and 12 (Mdm10p and Mdm34p, both of which are associated with the outer mitochondrial membrane [OMM] and Mdm12p, a cytosolic protein) as well as Maintenance of Mitochondrial Morphology 1 (Mmm1p, an ER associated protein)[114,117–121,125–127], and the regulatory protein GTPase EF-hand protein of mitochondria 1 (Gem1)[117,118,125], act to tether the ER membrane to mitochondria[113,114,117,118,120,121,126,129].

Aside from ERMES, a secondary protein complex, the endoplasmic reticulum protein complex (EMC), has been implicated in aiding the tethering of the ER to mitochondria at contact sites[114,119,125]; *EMCΔ* mutants display a loss of tethering in much the same way ERMES mutants

do[114], which can be rescued with the expression of a synthetic tether[113,114,118]. Mutants lacking 5 of the 6 subunits that make up the EMC are unable to grow on media that's devoid of fermentable substrates, suggesting completely non-functional mitochondria[114].

ER-mitochondria contact sites appear to be the primary method of lipid transfer between the two organelles. For example, the protein Lipid Transfer at Contact Site 1 (Ltc1), found localized to both ER-mitochondia and ER-vacuole contact sites, displays the capability to transfer sterols between organelles; *ltc1Δ* mutants under stress do not display the typical "ergosterol enriched" vacuolar domains, and conversely, an overexpression of Ltc1p yielded vacuolar membranes rich in ergosterol even in an absence of stress[119]. It should also be noted that *ERMESΔLtc1Δ* mutants are rendered completely unviable.

Although it's not entirely understood how, phospholipids are also transferred at ER-mitochondria contact sites [114–116,118,122,123,126,127]. Phosphatidylserine (PS) is transferred from the ER to mitochondria, where it becomes the substrate for phosphatidylserine decarboxylase 1 (Psd1), an inner mitochondrial membrane (IMM) enzyme that catalyzes the conversion of PS to PE[123,124,130,131]; a reaction that underpins the importance of ER-mitochondria contact sites, as PE, aside from being an important phospholipid in its own right, is a PC precursor as a part of the PEMT pathway[37,41,76,116,121,123,132].

1.2.2 Impact of Mitochondria on Metabolism of Lipids and Lipid Precursors

The mitochondrion is best known for its role in the generation of ATP, but it also has an important part to play in lipid regulation. First and foremost, as mentioned briefly, the IMM is home to Psd1p[123,124,130,131,133], a decarboxylase responsible for the biosynthesis of PE from its' precursor, PS. Psd1p is formed of two subunits, Psd1α and Psd1β, the former residing within the intermembrane space (IMS) and the latter acting as the IMM anchor[131]. *psd1Δ* mutants display a "petite" cell phenotype[121,124]. Psd1p is regulated by the IMM protease, Yeast mitochondrial escape protein 1 (Yme1p)[124]; *yme1Δ* knockouts yield increased Psd1p levels, and as such, higher PE.

The production of PE within the mitochondria serves multiple purposes, but primarily, it may be transferred back to the ER where it can undergo methylation by Cho2p and Ino3p as part of the CDP-DAG pathway to yield PC[37,76,116,121,123,132]. PC is the most prominent phospholipid in LD monolayers[1], and is indeed one of the primary constituent membrane phospholipids. Defects in PC biosynthesis give rise to the petite cell phenotype seen in *psd1Δ* mutant[121,124], as well as completely nonfunctional mitochondria[121]. A reduced PC composition of LD membranes, such as can be seen in *cho2Δ*, *opi3Δ* and other PEMT related protein mutants, leads to an SLD phenotype[37,134].

As well as PC synthesis, the IMM is the site of cardiolipin (CL) biosynthesis[43,114,135–137,118,121–123,125–127,131] by the enzyme Cardiolipin synthase 1 (Crd1)[127,135–137] CL is an important non-membrane phospholipid found exclusively within mitochondria[123,127] that constitutes to ~20% of mitochondrial phospholipid composition[136]. *crd1Δ* mutants, and therefore mutants

lacking sufficient CL, display a higher susceptibility to heat shock; prolonged heating causes a complete degeneration of the mitochondrial genome[135]. These mutants also show a drop in membrane potential, and a significant drop in respiratory function even when grown in glucose rich environments[135]. This is because CL's primary functions are the stability and organization of mitochondrial membranes and cristae, and to facilitate the formation of respiratory protein complexes such as the electron transport chain; interactions between CL and cytochrome C oxidase have been well documented[135,138,139]. It has also been documented that a *psd1Δcrd1Δ* double mutant, devoid in mitochondrial synthesis of both PE and CL, cells are rendered completely unviable, displaying the importance of these two mitochondrially driven phospholipid biosynthetic pathways[137].

1.3 Aims of this study

The role of LDs as storage for excess lipids has been well established, alongside its flexibility in relinquishing the stored TAG and SE to facilitate phospholipid synthesis and generally aid in lipid metabolism. However, a definitive role for lipid droplets within stress responses has not been fully established, despite studies indicating potential links to pro-longevity and LD proliferation under stressful conditions[12,13,134], as well as a platform for signalling processes[140,141]. Previous work done by the Gourlay lab (unpublished results) alluded to a similar role of LDs within the cell, and a potential link to the CWI signalling pathway. The purpose of this study was to determine the effect of stresses known to activate CWI signalling upon LDs within the cell, establish whether LDs and their regulation is linked to CWI signalling, and ultimately begin to elucidate how they may impact CWI signalling and cellular stress responses.

Chapter 2

Materials and Methods

2.1 Strains Used

2.1.1 Saccharomyces cerevisiae strains

Strain	Genotype	Plasmid Notes	Genetic background and source
CGY384 wt	Matα URA3-52, His3Δ200, Leu2-3112, Lys2-801, COF1::LEU2		DDY1252, D. Drubin
CGY386 Cofilin 1-5	Like CGY384, COF1-5::LEU2		DDY1254, D. Drubin
CGY1216	Like CGY384	PCG618 SLT2-GFP (overexpression)	CGY collection
CGY1218	Like CGY386	PCG618- SLT2-GFP (overexpression)	CGY collection
CGY1228	Like CGY384	PCG609- PKC1-GFP (overexpression)	CGY collection
CGY1230	Like CGY386	PCG609- PKC1-GFP (overexpression)	CGY collection
CGY1312 (*wt Lro1Δ*)	Like CGY384 Lro1Δ::KanMX		This study
CGY1315 *(cof1-5 Lro1Δ)*	Like CGY386, Dga1Δ::KanMX		This study
1318 *(cof1-5 Dga1Δ)*	Like CGY384, Dga1Δ::KanMX		This study
1321 *(wt Dga1Δ)*	Like CGY384, Dga1Δ:: URA3		This study

Table 2.1.1 ***S. cerevisiae strains used in this study***

2.1.2 Escherichia coli (E.coli) strains

Strain	Resistance	Plasmid Notes
DH5α 609	AMP	PVD67 (Pkc1-GFP) in PVD61 (2micron, GFP) URA3
DH5α 609	AMP	PFD146 PFL44 Mpk1-GFP(SLT2) URA 3

Table 2.1.2 *E. coli* strains used in this study

2.2 Media preparation

All growth media were prepared and then autoclaved at 121°C to ensure sterility. When growing cells overnight in the given media, yeast cells were cultured at 30°C in 50 ml glass boiling tubes whilst shaking at 200 rpm. *E.coli* cells were cultured at 37°C at 180 rpm.

2.2.1 Yeast Extract, Peptone, Dextrose Media (YPD)

Composed of 1% yeast extract, 2% peptone, 2% glucose. In the case of YPD agar plates, 2% oxoid agar was added.

2.2.2 Yeast selective dropout media (SD)

This media utilises the auxotrophic nature of the yeast strains used in order to select for cells that have taken up a particular plasmid or have successfully had target genes swapped for nutritional markers. The media is defined but deficient for a particular amino acid or nucleotide, and as such only cells that are capable of synthesising the missing elements are capable of growing.

Composed of 0.67% yeast nitrogen base media (YNB) without amino acids, 0.16% of yeast synthetic complete drop-out media supplement without uracil (Formedium), and 2% glucose. For SD agar plates, 2% Oxoid agar was added.

2.2.3 Yeast extract and tryptone (YT) media

Composed of 1.6% Bacto tryptone, 1% yeast extract, and 0.5% Sodium chloride (NaCl). For YT-ampicillin agar plates, 2% oxoid agar was added, the media was autoclaved, then cooled to 50^{o}C. 0.1% of the 100mg/mL ampicillin stock was added and mixed thoroughly before pouring.

2.3 Molecular Biology Techniques

2.3.1 Plasmid extraction from *E.coli*

5ml of YT media was inoculated with an *E.coli* strain containing a desired plasmid and grown overnight, shaking and at 37°C in the presence of a selective antibiotic. The following day, the culture was treated with a Qiagen QIAprep Spin Miniprep Kit, as a means of extracting and purifying the desired plasmid.

2.3.2 Design Of Primers For Gene Deletion

Target gene sequence +/- 1kb was downloaded as a .fsa file from *Saccharomyces* Genome Database (SGD) from the reference strain S228C and loaded into the program *Snapgene Viewer*. The required oligonucleotide sequences were added to the necessary template for each primer.

Forward primer- 50bp upstream of ATG start codon on forward strand +19bp complementary to DNA flanking selective marker

Reverse primer- 50bp downstream of end of gene reverse strand 5'-3' direction + 19bp complementary to DNA flanking selective marker

Control forward- 20bp, approx. 500bp upstream of ATG start codon. Begins with CG, ends in C or G. ~50% GC content

2.3.3 Amplification of gene disruption cassettes and genomic DNA

A Polymerase chain reaction (PCR) reaction was prepared within a thin walled PCR tube with total reaction volumes of 50µL and 20µL for disruption cassette amplification and genomic DNA amplification respectively. The ratios for PCR reactions used are as follows:

Reagent	**Percentage by volume (%)**
ddH_2O	70
10x PCR buffer (Invitrogen)	10
50mM $MgCl_2$	3
10mM dNTP	2
100µM forward primer corresponding to target gene	2
100µM reverse primer corresponding to target gene	2
5U/µL Taq polymerase (Invitrogen)	1
(Cassette amplification PCR only) 10-100ng/µL dilution of extracted plasmid containing desired selective marker	10
(Genomic DNA amplification PCR only)	10

10ng/µL extracted genomic DNA	

Table 2.3.3.1 PCR reagent quantities required for cassette amplification and genomic DNA amplification

These PCR reactions were then run on a Biorad C1000 thermal cycler with a cycle as follows:

Volume 50µL (Deletion cassette amplification)	**Volume 20µL (Genomic DNA amplification)**
Preheat lid to 105^{o}C	
95^{o}C for 300 sec	95^{o}C for 300 sec
95^{o}C for 40 sec	95^{o}C for 40 sec
56^{o}C for 40 sec	61^{o}C for 40 sec
72^{o}C for 100 sec	72^{o}C for 40 sec
GO TO 2, 34 cycles	**GO TO** 2, 34 cycles
72^{o}C for 900 sec	72^{o}C for 900 sec
8^{o}C forever	8^{o}C forever

Table 2.3.3.2 Thermocycler settings for each PCR reaction

The resultant product yielded by the 50µL reaction was an amplified deletion cassette, a linear strand of DNA that holds the selective marker required (either URA3 or KanMX) flanked either side by 34bp LoxP sites, and 50bp both upstream and downstream that correspond to regions flanking the gene targeted for disruption. It should be noted that, for this particular study, the recycling of the selective markers through LoxP cre recombinase activity has not been

carried out. The necessity of the 20µL reaction was for genomic DNA amplification to check for correct gene deletion, as described later in 2.3.8.

2.3.4 Purification of gene disruption cassette DNA

Deletion cassettes were amplified by PCR as previously described in 2.3.3. The amplified linear DNA was purified from the PCR reaction solution to concentrate the product as follows. Five PCR reactions were pooled together to a total volume of 250µL and 137.5µL 7M pH 7 ammonium acetate was added and incubated for 5 min at 65^{o}C before immediate cooling on ice for 5 min. 250µL chloroform was then added, mixed thoroughly, and then centrifuged at 13,000rpm for 2 min. The top layer supernatant was then removed with a pipette and placed into a separate clean Eppendorf tube. 500µL of 100% isopropanol was added to the supernatant which was then incubated at room temperature for 5 min, then spun at 13,000rpm for 5 minutes. The resulting supernatant was removed, and the pellet washed with 70% ethanol and dried, before being resuspended in 50µL autoclaved milli Q water. The result was a highly concentrated, purified linear DNA deletion cassette solution, devoid of the remainder of the reagents necessary for the PCR reaction.

2.3.5 Yeast transformation with linear DNA

S. cerevisiae were grown overnight in YPD media under standard growth conditions. After vortexing to ensure a uniform culture, 1mL was pipetted into an Eppendorf tube. The cells were centrifuged at 3000 rpm for 4 min. Meanwhile, an aliquot of single stranded carrier DNA (ssDNA) was incubated at 90^{o}C for 10 min to denature, and then placed on ice. Cells were pelleted by centrifugation at 4000 rpm for 3 min, the supernatant removed, and the pellet re-suspended in a transformation mix as follows:

240µL 50% Polyethylene glycol 4000 (PEG 4000)
36µL 1M lithium acetate (LiAc)
10µL 10mg/mL ssDNA
2.5µL 14.3M β-mercaptoethanol (BME)
20µL purified deletion cassette DNA
51.5µL Milli Q water

Table 2.3.5.1 BME transformation reagent list

The transformation mix was vortexed thoroughly to ensure a homogeneous mixture and incubated at room temperature for 20 min while subjected to gentle mixing, then treated to a 20 min 42^{o}C heat shock. The samples were then pelleted at 3000 rpm for 4 min and the supernatant removed. The pellet was resuspended in 200 µL of autoclaved Milli Q water, then plated onto the required selective plates. These plates were incubated for 3-5 days at 30 ^{o}C, and any colonies that arose were subsequently checked for correct gene disruption through genomic DNA extraction and PCR.

2.3.6 Yeast genomic DNA extraction

Colonies that grew upon the chosen selective media following deletion were re-streaked onto separate plates and labelled as individual clones. 3 mL of the necessary selective media was inoculated with each clone and grown overnight under standard growth conditions. 1ml of each of these cultures containing separate clones were pipetted into Eppendorf tubes, and centrifuged at 13,000 rpm for 1 min. The supernatant was removed, and the cells washed in 1mL Milli Q water. After washing, cells were centrifuged a second time at 13,000 rpm for 1 min. The supernatant was removed from the pellets, which were re-suspended in 500 µL lysis

buffer (100mM Tris pH 8, 50mM EDTA, 1% SDS). Each sample had a measured volume of acid washed glass beads added, bringing the total volume within the Eppendorf to 1.25 mL. The suspensions were vortexed for 1 min to lyse the cells. The liquid phase was then extracted from the Eppendorf, separating the lysed cell debris from the glass beads; a heated needle was used to pierce the bottom of the Eppendorf, which was then placed within a second Eppendorf, and subjected to a centrifugal force of 2000 rpm for 30 sec. 275µL of 7M ammonium acetate (pH 7) was then added to the cell lysate. This was then incubated at 65^{o}C for 5 min, and then a further 5 min on ice. 500µL of chloroform was then added to each sample, followed by brief mixing using a vortex, and then centrifuged at 13,000 rpm for 2 min. The upper phase was removed and placed into a separate Eppendorf tube and 1mL of isopropanol was added and the solution briefly mixed by inversion followed by incubation at room temperature for 5 min and centrifugation at 13,000 rpm for 5 min. The isopropanol acts to precipitate genomic DNA out of solution. The supernatant was removed from the genomic DNA pellet, which was then washed in 70% ethanol. The ethanol was removed, and the pellet was dried and resuspended in 50µL of autoclaved milli Q water.

2.3.7 Biodrop analysis of DNA extracted from yeast cells

In order to establish the success of the genomic DNA extraction, the concentration and purity of the genomic DNA solution was checked using a Serva Biodrop µLite UV/Vis spectrophotometer. The biodrop spectrophotometer analyses the samples at 260nm, 280nm, and 230nm wavelengths.

2µL of water was used to blank the machine. 2µL of DNA sample obtained from 2.3.6 was then loaded between the probes of the machine, and the absorbances at the above

wavelengths recorded, yielding a concentration in ng/µL and 2 measures of purity: the A260/A280 ratio and the A260/A230 ratio.

The A260/A280 ratio is used to discern purity of a DNA sample by comparing an absorbance wavelength that detects nucleic acids (260nm) and protein (280nm). A sample with an A260/A280 ratio between 1.8-2.1 is considered pure with negligible protein contaminants.

The A260/A230 ratio is also used as a measure of purity to discount the presence of contaminating phenols and other compounds. This value should be approximately 2 to denote a pure sample.

3.3.8 PCR check of gene disruption

Each purified genomic DNA extraction sample generated in 2.3.6 was diluted to a concentration of 10 ng/µL and subjected to a PCR reaction to determine correct insertion of the disruption cassette. The PCR reaction was of 20µL total volume, and the reagent quantities were described in Table 2.3.3.1, and the thermocycler settings described in Table 2.3.3.2.

The sequence used to design the control forward primer used for the PCR reaction was located approximately 500 bp upstream of the target gene, as described in 2.3.2. while the reverse primer was located within the selective marker used for the deletion.

2.3.9 Gel electrophoresis of DNA

A 1% agarose solution was prepared (1g agarose, 100mL 1x TAE [98% ddH_2O, 2% 50x TAE-recipe below]), and boiled to fully dissolve the agarose.

50x TAE- 10% 0.5M EDTA, 5.71% glacial acetic acid, 2M Tris-base.

1µL of 20mg/mL ethidium bromide was added to the agarose solution and mixed gently. Ethidium bromide is a DNA chelating agent that is detectable upon application of UV light, and therefore may be used to detect the presence of DNA bands on a gel. 40mL of the liquid agarose solution was poured into a mould with a comb with the desired amount of wells. The agarose gel was allowed to set, and the comb was carefully removed to form the wells within the gel. The gel was placed into an agarose gel tank, and immersed in TAE- ethidium bromide buffer (1x TAE, 0.5µg/ml ethidium bromide). 4µL of 6x blue/orange loading dye (Promega) was added to 18µl of each sample of the control PCR reactions. The samples were loaded into individual wells in the gel. In a separate well, 5µL of 1kb+ generuler DNA ladder (thermofisher) was added. The gel was run at 90 V for 30 min before visualisation using a Syngene GBox XX6 imaging system.

2.3.10 Yeast plasmid transformation

This protocol allowed for the insertion of plasmids to express GFP-tagged proteins within the *S. cerevisiae* strains used in this study. Cells were grown overnight in YPD under standard growth conditions. 1ml of the resultant cell culture was pipetted into an Eppendorf tube, and centrifuged at 4000 rpm for 3 min. The supernatant was removed from the pellet, which was then washed and resuspended in 1mL 1x Tris-EDTA (TE) buffer (10x TE buffer- 10% 1M Tris-HCL pH 8, 2% 0.5M EDTA pH 8). The cells were centrifuged again at 4000 rpm for 3 min, and the TE buffer was removed from the pellet. 1mL of TE-LiOAc (lithium acetate) (80% Milli Q water, 10% 10x TE, 10% 1M LiOAc) was added and the pellet was resuspended. The cells were centrifuged once more at 4000 rpm for 3 min. The TE-LiOAc was removed from the pellet, and the washed pellet was re-suspended in 0.1mL TE-LIOAc. Meanwhile, an aliquot of 10mg/ml ssDNA was boiled at 90^{o}C for 10 minutes and then placed on ice. 15µL of the ssDNA was added to the cells suspended in TE-LiOAc, followed by 2µL of 1:10 plasmid DNA (10-

100ng/µL). 700µL 40% PEG4000 (40µL 50% PEG4000, 5µL 1M LiOAc, 5µL 10x TAE) was added to the sample and mixed thoroughly. The mixture was then incubated at room temperature for an hour, whilst rotating gently. Following the room temperature incubation, cells were treated to a 15 min heat shock at 42^{o}C. The transformed cells were then centrifuged at 4000 rpm for 3 min, and the supernatant was fully removed. The cells were then resuspended in 200µL sterile water. The cells were plated on the necessary selective plates (SD-URA agar plates) and incubated at room 30 ^{o}C for 3-5 days, then checked for colony growth to assess successful transformation.

2.4 Protein Methods

2.4.1 Antibodies used in this study

The use of antibodies was necessary for the detection of specific proteins in western blot analysis. The antibodies used in this study were as follows:

Antibody	Dilution	Source
Phospho-p44/42 MAPK (Erk1/2) Rabbit monoclonal antibody- Primary antibody for phospho-Slt2 detection	1:1000	Purchased from Cell signalling technology, Inc
α-Yeast act1 Goat monoclonal antibody- Primary antibody for Act1 loading control	1:2000	A kind gift from John Cooper, Washington University
Anti-Rabbit IgG HRP- Secondary antibody for detection of act1	1:3000	Sigma Aldrich, product number A 8275
Anti-sheep IgG HRP- Secondary antibody for detection of act1	1:3000	Sigma Aldrich, product number A3415

Table 2.4.1 Antibodies used within this study

2.4.2 Cell wall stress and whole yeast protein extraction for Western blotting

Cells were grown in 3mL YPD under standard growth conditions for 24h before separating culture into two, one to act as a control and the other to undergo stress treatment. Stressed samples were subject to a 200µM calcofluor stress (10µL of 20mM calcofluor in 990µL cell culture) for 2 h in the 30 ^{o}C shaking incubator prior to extraction, whereas the control samples received no calcofluor treatment but were still incubated in the same way.

The OD_{600} of each sample was measured using an Eppendorf biospectrometer and from this value, the volume of culture required to provide approximately $1x10^8$ cells was calculated. $1x10^8$ cells were harvested by centrifugation at 4000 rpm for 3 min, and the supernatants were removed. The pellet was resuspended in 200µL lysis buffer (0.1M Sodium hydroxide, 0.05M EDTA, 2% SDS, 2% BME), and then heated at 90^{o}C for 10 min. 5µL of 4M acetic acid was added, and the sample was vortexed for 30 sec, and incubated for an additional 10 min at 90 ^{o}C. 50 µL of loading buffer was then added (0.25M Tris-HCL pH 6.8, 50% glycerol, 0.05% bromophenolblue) to each sample. The samples were then centrifuged at 4000 rpm for 3 min to clear the lysate and cell debris, and then kept on ice prior to loading them onto an SDS-PAGE gel.

2.4.3 Protein Gel Electrophoresis

Following protein extraction, protein samples were subject to SDS-PAGE electrophoresis, which separates charged proteins by size. A gel tank was assembled, housing 2 Invitrogen nupage 4-12% Bis-Tris gels . The inner chamber of the tank was filled with 1x MOPS (5% 20x Novex MOPS SDS running buffer), and the outer chambers were halfway filled with MOPS buffer. 10µL of the supernatant of each prepared protein sample was pipetted into a separate well. 5µL of pageruler prestained protein ladder was added to wells at the start and in the

centre of the gel. The gels were run at 120 volts for 90 min, until the dye front was approximately ¾ of the way down the gel.

2.4.4 Semi Dry Transfer of proteins to PVDF (Western Blotting)

Two 8cm x 9cm rectangles of Whatman's extra thick blotting paper were cut, as well as a 8cm x 9cm piece of Polyvinylidene difluoride membrane (PVDF, Roche). The PVDF membrane was wet thoroughly with methanol, and then placed in 1x transfer buffer (100ml methanol, 350ml water, 50ml 10x transfer buffer [29g glycine, 58g tris base, 40µL 10% SDS, made up to 1L]) to soak for 10-15 min. The blotting paper was also soaked in transfer buffer. A Bio-rad Trans-blot Turbo Transfer system was to perform the western blot semi-dry transfer. A piece of wettened blotting paper was placed upon the bottom electrode within one of the housings, and a roller was used to roll out the bubbles. The PVDF membrane was placed carefully on top of the blotting paper, then marked in the corner to ensure correct orientation was maintained throughout. The air bubbles were then removed from between the PVDF and the blotting paper with a roller. The gel was removed from the gel tank and buffer, and the plastic casing housing the gel was pried open using a gel knife. The wells were carefully cut from the rest of the gel using a razor blade, and the gel was released from the plastic housing by cutting into the groove at the bottom of the gel. The gel was then placed on top of the PVDF membrane, and a second layer of blotting paper was placed on top of the gel. The whole structure was rolled one final time to ensure there were no air bubbles, and the lid, housing the upper electrode, was carefully placed on top and then locked into place. Both gels were treated in the same way and run through the semi-dry transfer machine concurrently, as there were two housings each with their own set of positive and negative electrodes. The transfer took place at 25 volts and 0.5 amps for 30 min.

2.4.5 Coomassie staining of SDS-PAGE gel

Following the semi-dry transfer, the SDS-PAGE gel was stained to determine the effectiveness of the transfer. The gel was washed briefly 3 times in 1x PBS (10x PBS pH 7.4- 8% NaCl, 0.2% potassium chloride[KCl], 1.44% Sodium phosphate dibasic [Na_2HPO_4], 0.24% Potassium phosphate dibasic [KH_2PO_4), and then submerged in Coomassie blue stain (0.25% Brilliant Blue, 50% methanol, 10% glacial acetic acid) whilst gently mixing on a Luckham R100 rotatest shaker for 30 min. The Coomassie blue stain was removed from the gel, which was then submerged in de-staining (40% methanol, 10% glacial acetic acid) solution and gently rocked for 15 min. This de-stain was removed and replaced with fresh de-stain, and allowed rocked gently for a further 10 min. This step was repeated until the stain was sufficiently removed from the gel and only a banding pattern of stained protein was visible.

2.4.6 Western Blot - Protein detection

Proteins transferred to PVDF membrane were probed for specific proteins as follows. PVDF was rinsed three times in PBS-tween 20 (PBS/T) (10% 10x PBS, 90%, 0.2%Tween 20), and then submerged in blocking solution (5% dried skimmed milk powder in PBS/T) and placed on the rotatest shaker for 45 min at room temperature. Meanwhile, 3mL of blocking solution was placed into a 50mL falcon tube, and the necessary amount of primary antibody was added (see 2.4 above for required dilutions), and then mixed gently. The membrane was briefly rinsed with PBS/T to remove excess blocking solution, and the membrane was then placed inside the falcon tube with the proteins facing inward, and the falcon tube sealed. The membrane was bathed in the primary antibody overnight at 4^oC The membrane was briefly rinsed with PBS/T twice to remove excess blocking solution and primary antibody, then submerged in PBS/T and shaken gently for a 15 min wash, then subsequently two more 5 min washes with PBS/T to ensure all unbound antibody was removed. A second 50mL falcon tube

was prepared with 5mL blocking solution containing the necessary amount of Horse radish peroxidase conjugated secondary antibody. The membrane was placed into a clean 50ml falcon tube, protein side facing inward, and incubated at room temperature on a roller mixer for 30 min. The membrane was then washed three times in PBS/T for 15, 5 and 5 minutes, but with an additional 5 minute wash in PBS/T. The membrane was then stored in PBS buffer.

2.4.7 Enhanced chemiluminescence (ECL) detection of proteins on Western blot

The following solutions were prepared prior to detecting the proteins on the PVDF membrane:

Solution I- 1% 250mM luminol, 0.44% 90mM p-coumaric acid, 10% 1M Tris-HCl pH 8.5

Solution II- 10% 1M Tris-HCL pH 8.5, 0.064% 30% H_2O_2

The presence of the proteins was detectable through the enzymatic activity of HRP conjugated to the secondary antibody. 5mL of solution 1 and solution 2 were mixed together, and then poured evenly across the top of the membrane. The membrane was left in this solution for 1 min and placed within a plastic sheet, rolled to remove excess liquid and air bubbles. The Syngene G Box XX6) was then used to detect luminescence.

2.4.8 Stripping of Western Blot

The PVDF membrane to be stripped was washed in PBS and then soaked in Restore western blot stripping buffer (Thermo Scientific) and gently shaken for 30 min. Following this, the membrane was rinsed with PBS/T and subject to 15, 5 and 5 minute wash steps, and could then be re-blocked and re-probed with different antibodies as necessary.

2.5 Microscopy Techniques

2.5.1 Sample preparation

Cells were grown overnight in 3mL of appropriate selective medium under standard growth conditions, and subsequently used to inoculate 3mL of YPD at an OD600 of 0.1. Cells were then grown under standard growth conditions for 24 h. The culture was divided into 1mL aliquots and treated to stresses as follows:

Control- 30^{o}C incubation for 2 h

Oxidative stress- 1% of 1mM H_2O_2 for 2 h

Calcofluor stress- 1% of 10mM Fluorescent brightener 28 (Calcofluor white M2R, Sigma Aldrich)

Copper Sulphate stress- 1% of 1mM copper sulphate for 2 h

Heat stress- 37^{o}C for 2 h

2.5.2 LD540 staining of cells

In order to visualise the lipid droplets within cells, the stain LD540 was used. A 200µL aliquot of cell culture was pipetted into an Eppendorf tube, and 0.2µL of 0.5mg/mL LD540 was added and mixed briefly through inversion of the eppendorf. These samples were left for 5 min and then centrifuged at 10,000 rpm for 2 min. The supernatant was removed from the stained cells and they were resuspended in 50µL H_2O.

2.5.3 Preparation of slides

The samples µL were vortexed thoroughly, and 2µL of sample was placed upon a clean, clear microscope slide. A 20mm by 20mm cover slip was carefully lowered on top of the sample.

2.5.4 Fluorescence microscopy

To observe cells, an Olympus IX81 inverted microscope was used. The light source was provided by a CooLED pE4000 illumination system, and all images were captured with an Andor's Zyla **4.2** PLUS sCMOS camera. Cells were viewed using an olympus 100x objective lens. A small droplet of Olympus Immoil- F30CC immersion oil was applied to the lens, and the sample slide inverted and placed upon the stage, and microscopy was carried out. LD540 was viewable under the RFP channel with the excitation/emission wavelengths of Cells with GFP tagged proteins were observable using the GFP channel with excitation/ emission wavelengths of 488/512nm. All microscopy was repeated in triplicate to ensure observations were accurate. Images were processed using ImageJ FIJI. Z-stack images taken were compressed into max projections of fluorescence.

2.5.5 Measurement of parent cell diameter using ImageJ

The global scale for the images was set for the images taken at 100x objective lens as defined by the specifications of the camera used. To measure diameter, a line was drawn across the widest portion of a mother cell, and the measure function was used, providing a distance in µM. This was performed for 150 cells per strain, in triplicate, and thus an average cell diameter could be determined.

2.6 Analysis of growth and viability in *S. cerevisiae strains*

2.6.1 Propidium Iodide (PI) staining to quantify necrosis using flow cytometry

PI is a DNA chelating agent that may be detected with the use of a flow cytometer (FACSCalibur, BD Biosciences). PI does not readily permeate into living cells, and thus when not bound to DNA, has an emission/excitation maxima of 493/636nm respectively. When bound to DNA, as it is able to do within necrotic cells, the excitation/emission maxima shifts to 535/617nm. This difference in fluorescence provides the means for detection of the proportion of necrotic cells within the population. *S.cerevisiae* was grown overnight in appropriate media and under standard conditions, and then inoculated to OD_{600} 0.1 within a 48 well plate. The cultures were then incubated for a total of 24 h at 30°C and shaken constantly and consistently. Cells were either treated with 200 µM calcofluor stress, a 100µM cercosporamide treatment, or neither, as per the requirements of the experiment in question. 30µl of cell culture was added to a FACS tube along with 500µl PBS with 0.004% 1mg/mL PI. Brief mixing through vortexing ensured sufficient distribution of the cells throughout the buffer. A negative control was created by adding cell culture to PBS with 0% PI. As a positive control, standard cells were treated with a 65°C heat shock for 10 min, and PI stained in the same way as the other samples. A total of 30,000 cells were analysed per sample. Using the FL2 emission filter the proportion of PI stained cells within the population could be calculated.

2.6.2 CFU Assays as a measure of viability

Yeast strains were grown in 3 mL of their respective selective medium overnight under standard growth conditions. These strains were then used to inoculate 300 µL of YPD media, in technical triplicate, for each condition required, within a 48 well plate. These strains were

allowed to grow for a total of 24 hours. Cells were subjected to (100µM) cercosporamide or 200 µM calcofluor stress at the 22 h timepoint and incubated for a further 2 h before viability was assessed. At the 24 h time point, a 1:100 dilution was made of each cell culture (10µL cell culture, 990µL Milli Q water) in sterilised 1.5mL eppendorf tubes. Samples were then vortexed thoroughly to ensure even dispersal of cells. To accommodate for the flocculation phenotype associated with the cofilin 1-5 background, each 1:100 dilution was then sonicated using a thin probe on an MSE Soniprep 150 at an amplitude of 4 microns for 10 sec per sample. The probe was thoroughly cleaned with ethanol between each sample to avoid cross contamination. Samples were vortexed, then a 1:10,000 dilution was created from the 1:100 dilution (10µL 1:100 sample, 990µL Milli Q water) in fresh, sterile 1.5mL Eppendorf tubes. 10µL of the 1:100 dilution was applied to a clean haemocytometer, which was used to count the number of cells. From the counted value, the number of cells in the original sample was calculated, and the volume of 1:10,000 sample dilution required to plate 250 cells was subsequently calculated. 250 cells of each culture were plated onto YPD plates and spread thoroughly using a sterilised glass spreader. These plates were then incubated for 48 h at 30^{o}C. At 48 h colonies were counted and the percentage of plated viable cells, or colony forming units, calculated.

2.6.3 Growth curve analysis of yeast strains

The growth of all strains were observed over the course of 24 h on a BMG Labtech SpectroStar nano plate reader. Cells were grown in in 3mL of YPD overnight under standard growth conditions. Within a 48 well plate, 300µL of YPD was inoculated to an OD_{600} of 0.1 with technical triplicates. A script was run with the following parameters in order to measure growth rates of the strains:

Excitation	600 nm
Shaking Frequency	400 rpm
Shaking Mode	Double Orbital
Additional Shaking Time	120 sec
Temperature	30^{o}C

One full cycle consisted of 120 seconds of the above shaking, followed by a the reading of OD_{600} of each of the wells, and a subsequent 120 second shake and read.

The strains' rates of growth were measured in triplicate. From each biological repeat, doubling times were calculated within excel at the maximum rate of growth, and lag times for each strain was also calculated.

Chapter 3

Results

3.1 Creation of *dga1Δ* and *lro1Δ* mutants

Deletions of the *DGA1* and *LRO1* genes were performed in both the wild type and *cof1-5* mutant backgrounds. Using the Cre-Lox system, genes may be replaced by selective markers such as the *URA3* gene[142], by allowing a *URA3* mutant strain to grow on media lacking uracil.

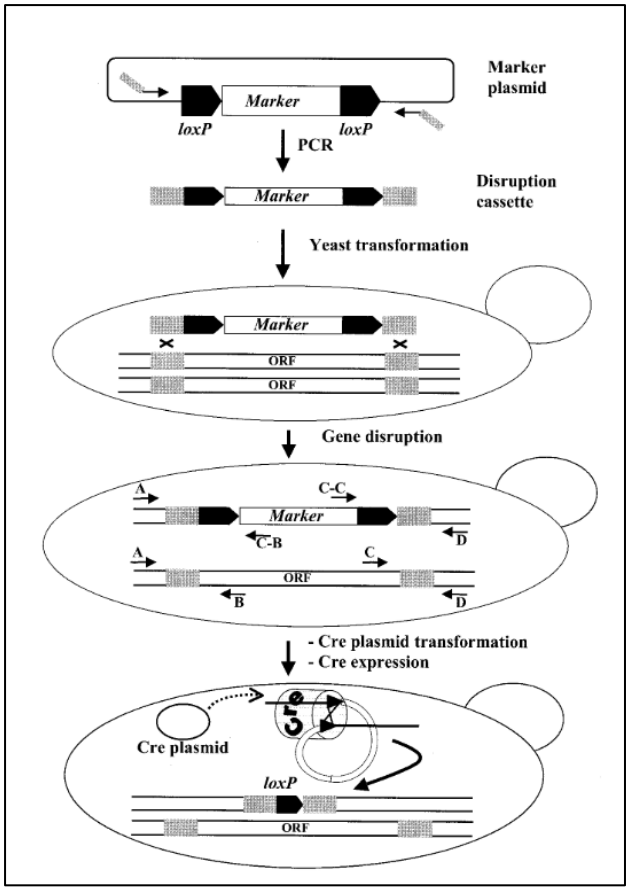

Figure 3.1.1 LoxP/Cre gene disruption The process of LoxP/Cre gene disruption utilises a selection marker gene such as *URA3* or KanMX, flanked by 34bp LoxP sequence regions each side. These regions of plasmid are integrated into strand of linear DNA using forward and reverse primers specific to sequences that flank the selection marker gene. These primers contain regions complementary to the loxP sites, coupled with 50 bp that matches the 5' upstream and downstream regions of the target gene. PCR allows for the creation of this disruption cassette. This linear DNA may then be transformed into desired yeast strains, and

successful integration through homologous recombination may be then checked with the use of PCR. The presence of the loxP regions either side of the inserted gene allows for easy removal of the marker by expression of Cre recombinase from an additional plasmid if necessary, allowing for recycling of the selective marker for further use[142]. Figure sourced from Gueldener *et al*[142].

The first stage of deletion using this method requires amplification of the deletion cassette. The majority of the deletions were created with the KanMX gene as a selective marker, which provides *S. cerevisiae* with a resistance to the drug, geneticin (G418) at a concentration of 200µM in YPD agar plates. Deletion of *DGA1* in a wild type background , however, was created using the *URA3* gene; a gene that provides an auxotrophic strain the capacity to synthesise its own uracil. A PCR reaction was run with forward and reverse flanking primers specific to the genes to be deleted, namely *DGA1* and *LRO1*.

It was necessary to purify the amplified deletion cassettes from the remainder of the PCR reagents and loose primers. To achieve this I pooled a number 5 duplicate PCR reactions and carried out an isopropanol DNA precipitation so as to concentrate the linear DNA. Their concentration was then checked using a biodrop (Serva) to ensure a concentration of ~100ng/µL.

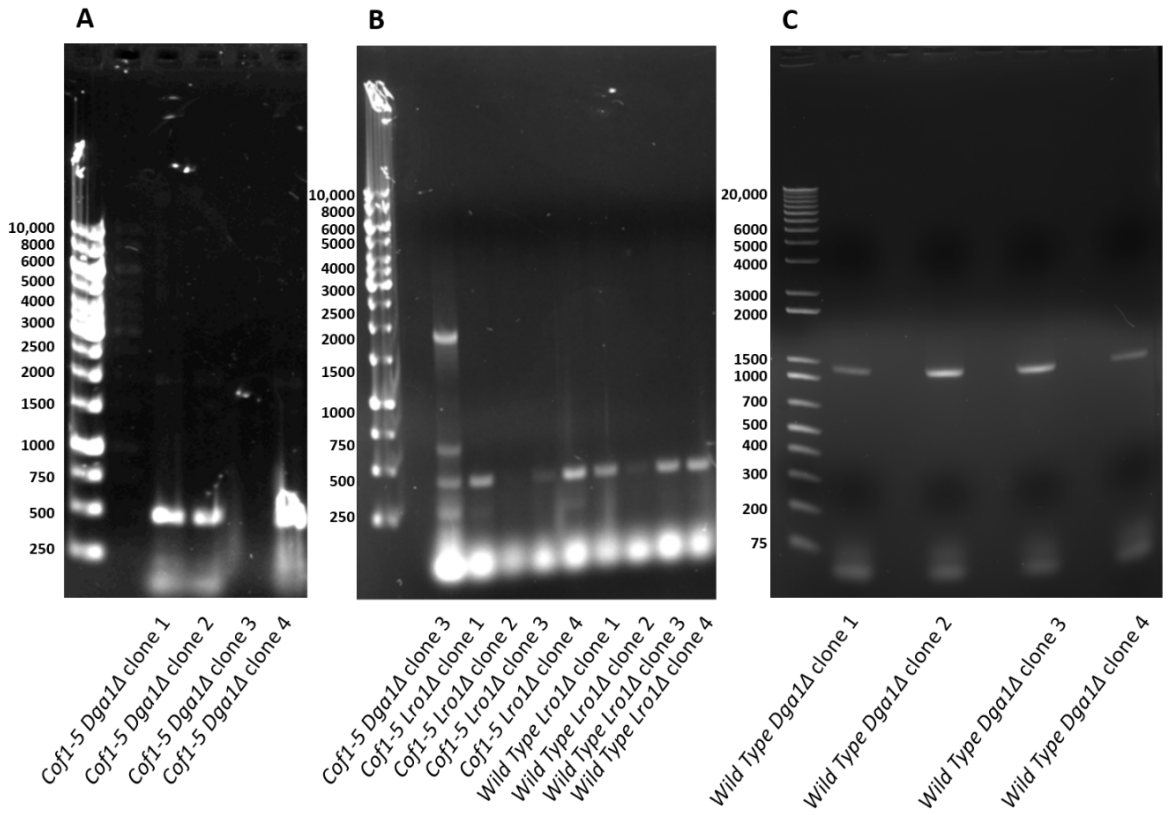

Figure 3.1.2 Confirmation of gene deletion Genomic DNA extracted from colonies that grew under selective conditions following transformation were subjected to PCR with the control forward primer and the reverse primer complementary to the chosen selective marker gene. These PCR reactions were then run on a 1% agarose gel to confirm the presence of the amplified DNA strand. **(A)** An agarose gel containing 4 clones of the putative *cof1-5 Dga1Δ* strain, checking for the presence of the *KanMX* gene at ~500bp with generuler 1kb ladder **(B)** An agarose gel containing both wild type and *cofilin 1-5 lro1Δ* strain clones to check for the presence of the *KanMX* gene at ~500bp with generuler 1kb ladder **(C)** An agarose gel containing *the wild type lro1Δ* clones; the gel checks the presence of the *URA3* gene at ~1500bp with generuler 1kb+ ladder.

Transformations using a protocol which utilises BME to aid the uptake of DNA, were used to insert the deletion cassette; the necessity of this transformation was to overcome the thicker fungal cell wall *in cofilin 1-5*. The transformed cells were plated on the necessary selective plates and left to incubate for 3-5 days. Any colonies present on these plates were then subjected to a genomic DNA extraction. In order to validate the correct insertion of the selective marker in place of the *DGA1* and *LRO1* genes, PCR was performed using a control forward primer of approximately 500 bp upstream of the gene, and a reverse primer specific to the loxP site, in order to amplify the successfully deleted region. These PCR products were then run and visualised on agarose gel, whereby amplified DNA may be detected with ethidium bromide. The presence of a band of approximately 500bp in size, as seen in figure 3.0.3, confirmed the correct insertion of selectable markers in place of the *DGA1* and *LRO1* genes, yielding *dga1Δ* and *lro1Δ*. Three of the four clones tested had a correct insertion of the KanMX gene to replace the *DGA1* gene in the cofilin1-5 background (Figure 3.1.2). One of these clones did not yield a correct band on the gel; possibly as a result of an unsuccessful PCR reaction, or an incorrect insertion of the gene. Clone 3 of the *cofilin 1-5 dgaΔ* candidates was rechecked for insertion of the deletion cassette into the genome; while a band is present at approximately 500, there were also a number of non-specific bands present in this particular clone. The cofilin 1-5 *LRO1ΔLRO1Δ* clones, again, showed a 75% success rate when run on an agarose gel. Wild type *LRO1ΔLRO1Δ* appeared to have successful insertion of the KanMX gene in all four clones (Figure 3.1.2).

3.2 The effects of *DGA1* and *LRO1* disruption on growth in wild type and *cof1-5* cells

The two strain backgrounds used in this project were wild type and the cofilin 1-5 mutant. The cofilin 1-5 mutant was created utilising site directed mutagenesis in order to introduce a point mutation to yield a *S. cerevisiae* strain with defective Cofilin1 protein. The strain was constructed by introducing this mutation into a heterozygous cof1/COF1 strain by homologous recombination and sporulating the diploid to yield haploid *cof1-5* cells[143]. This approach was necessary as the COF1 is essential. The wild type background used had the fully functional COF1 gene reintroduced into the cof1/COF1 heterozygous strain in the same way. The cofilin 1-5 mutation leads to a reduction in the dynamic nature of the F-actin cytoskeleton[143]. The effects of this are as such; cofilin is necessary for the breakdown and general regulation actin cytoskeleton, which in turn allows for correct progression through the cell cycle. We observed that cells expressing the cof1-5 mutation displayed flocculation, vacuolar fragmentation, a thickened cell wall that was caused by constitutive activation of the cell wall integrity pathway (Unpublished observations from the Gourlay lab). Cells expressing the cof1-5 allele also display an increased number of lipid droplets (Gourlay lab, unpublished results). We wished to determine whether lipid droplets played a role in the activation of the CWI pathway or the other phenotypes observed in cof1-5 cells, hence the necessity for the generation of the *dga1Δ* and *lro1Δ* strains.

The reason for looking at the growth rates of any and all strains created during this project were twofold. Firstly, the signalling pathway that has been focussed on, the cell wall integrity pathway of MAPK signalling, is known to regulate progression of the cell cycle during growth

phase[91]. Secondly, lipid droplet formation is central to the control of fatty acid and phospholipid metabolism, a requirement for growth and viability.

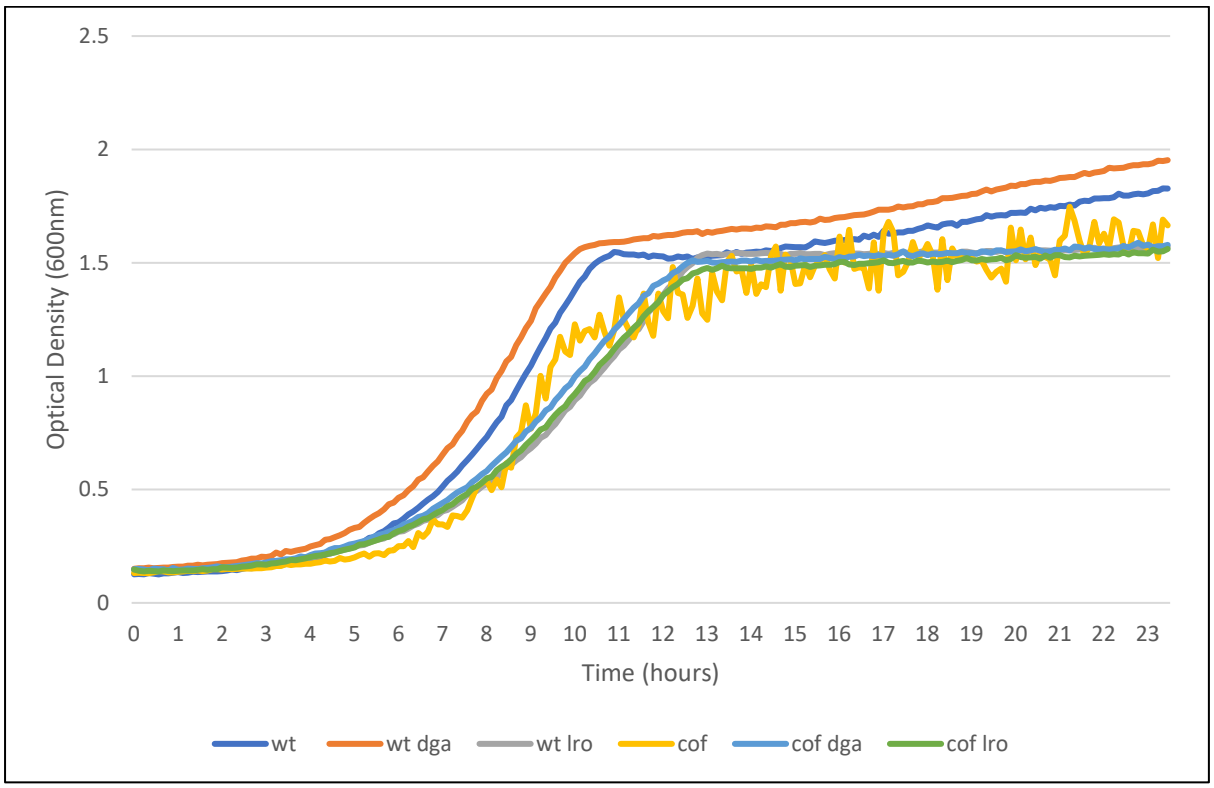

Figure 3.2.1 A graph to show the growth curves of *dga1Δ* and *lro1Δ* in both backgrounds strains were grown in YPD overnight under standard growth conditions, and then inoculated to 0.1 with technical triplicates within a 48 well plate. The OD_{600} of these strains was measured periodically to yield a growth curve. These experiments were completed with three biological replicates, in triplicate.

Each of the strains in this study were grown overnight in YPD and then used to inoculate fresh YPD to an OD_{600} of 0.1; this ensured that all cells were at the exact same start point, with precisely the same nutrition available to ensure no other variables that may affect growth. The growth of these strains was then observed over the course of 24 hours (fig 3.2.1); using the plate reader to observe the OD_{600} of each strain approximately every 7 minutes. From these analyses the doubling times and lag phases of each strain was calculated in order to be compared to that of the wild type and to the respective background strain.

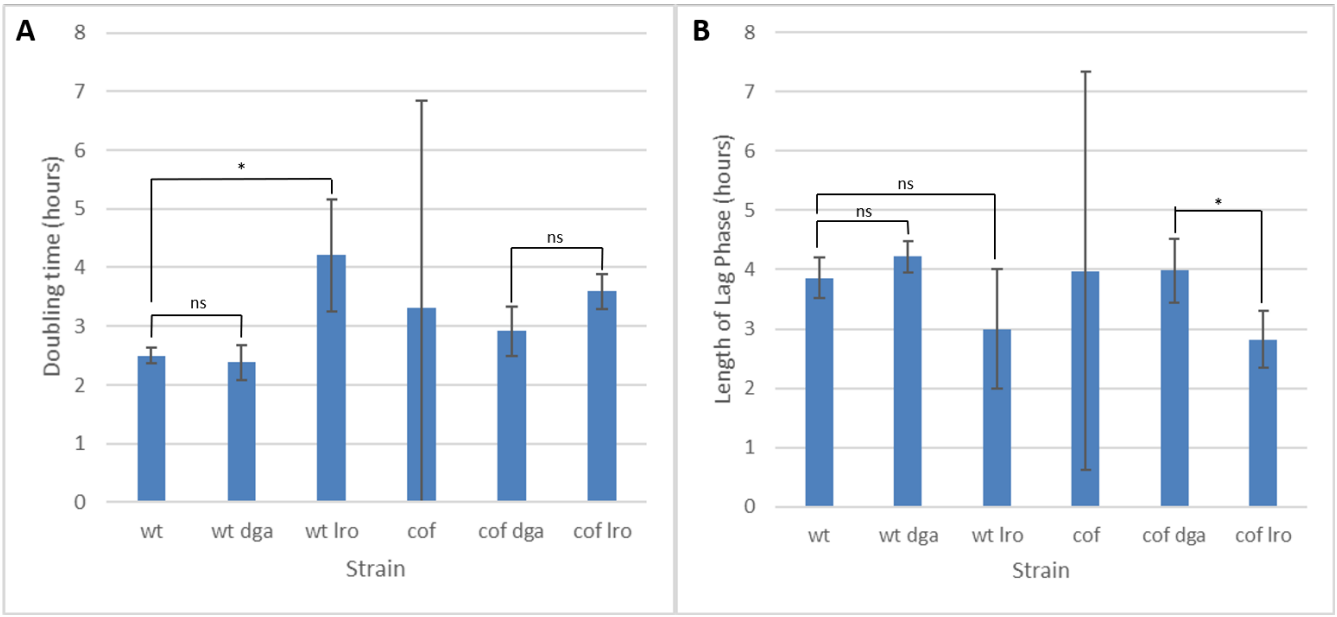

Figure 3.2.2 Analyses of the growth curve data (A) a bar graph displaying the doubling average doubling time of each strain at its fastest, within the log phase of growth at optimal growth conditions **(B)** a bar graph displaying the lag phase of each of the strains, or the period of time after inoculation that it takes for the cells to adjust to their new growth medium.

Comparing the wild type to the cofilin 1-5 mutant background, the growth defects of the cofilin 1-5 were readily apparent; the fluctuations in growth seen can be attributed to the

tendency for cofilin 1-5 cells to flocculate. Due to this it proved extremely difficult to calculate the correct lag and doubling times of this strain; as such the degree of variability while processing these samples was high.

There was no significant difference in lag phase or doubling time when comparing the *DGA1* and *LRO1* deletion in the wild type background to their parental strain (fig 3.2.2). The deletion of *LRO1* led to a doubling time of approximately 2 h longer than that of the wild type, but showed no significant change in lag time.

Due to the flocculation of the cofilin 1-5 mutant it proved challenging to compare the doubling times of the *DGA1* and *LRO1* deletions in this background. However, cofilin 1-5 *lro1Δ* cells displayed a significantly reduced lag time when compared to that of cofilin 1-5 *dga1Δ*, comparable with that of the wild type *lro1Δ* strain (fig 3.1.2b). The smoothing of the dga1*Δ* and *lro1Δ* growth curves is also indicative of a loss of flocculation, suggesting that loss of these genes may reduce CWI signalling activity. This effect could also observed by observing cultures after 24 h growth (fig 3.2.3).

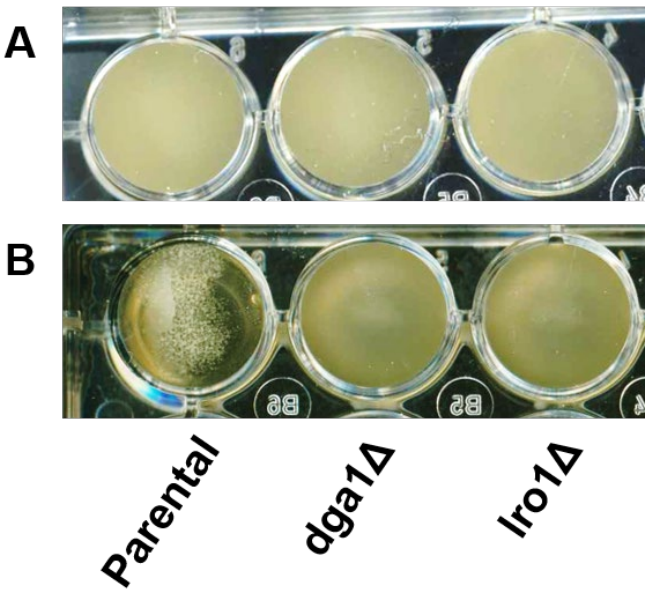

Figure 3.2.3 Demonstration of the cofilin 1-5 flocculation phenotype Images taken after 24 h growth. **(A)** 24 well plate containing 1mL parental, d*ga1Δ* and *lro1Δ* in wild type background **(B)** 24 well plate displaying 1mL *cof1-5* background and deletions

3.3 Analysis of wild type and *cof1-5* background by fluorescence microscopy

To observe lipid droplets within each strain, the cells were stained with LD540, a fluorescent dye that specifically binds the neutral lipids that make up the core components of the lipid droplets. After centrifugation, resuspension and mounting upon slides, the characteristics of these cells could be observed using fluorescence microscopy (fig 3.3.1).

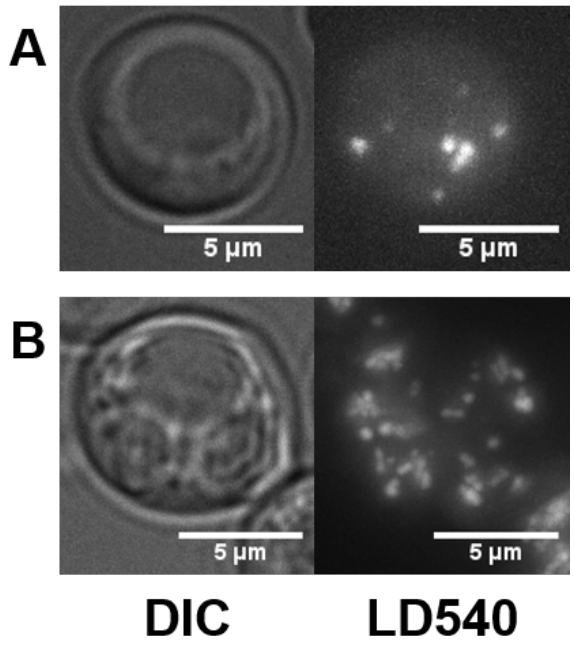

Figure 3.3.1 A comparison of lipid droplet formation in wild type and *cof1-5* cells Cells were observed after 24 h growth in YPD. LD540 staining allowed for imaging of lipid droplets in the RFP channel **(A)** A typical wild type cell during stationary phase **(B)** A cofilin 1-5 mutant cell during stationary phase

Microscopic analyses of the cofilin1-5 background displays larger-than-normal cells with fragmented vacuoles (figure 3.3.1). In these cells, LD540 staining revealed a significant increase in the number of lipid droplets as had been described previously (Dr. Patrick Rockenfeller, Gourlay lab, unpublished results).

As cof1-5 cells are under constitutive cell wall stress we wished to determine whether an increase in lipid droplet number forms part of a normal cell wall stress response. To do this lipid droplet number was calculated from biological triplicate cultures within the wild type

strain when exposed to stress during stationary phase. These cells were subjected to a variety of stresses known to activate CWI signalling; oxidative stress in the form of hydrogen peroxide, a 37^{o}C heat shock, and a cell wall stress in the form of calcofluor white.

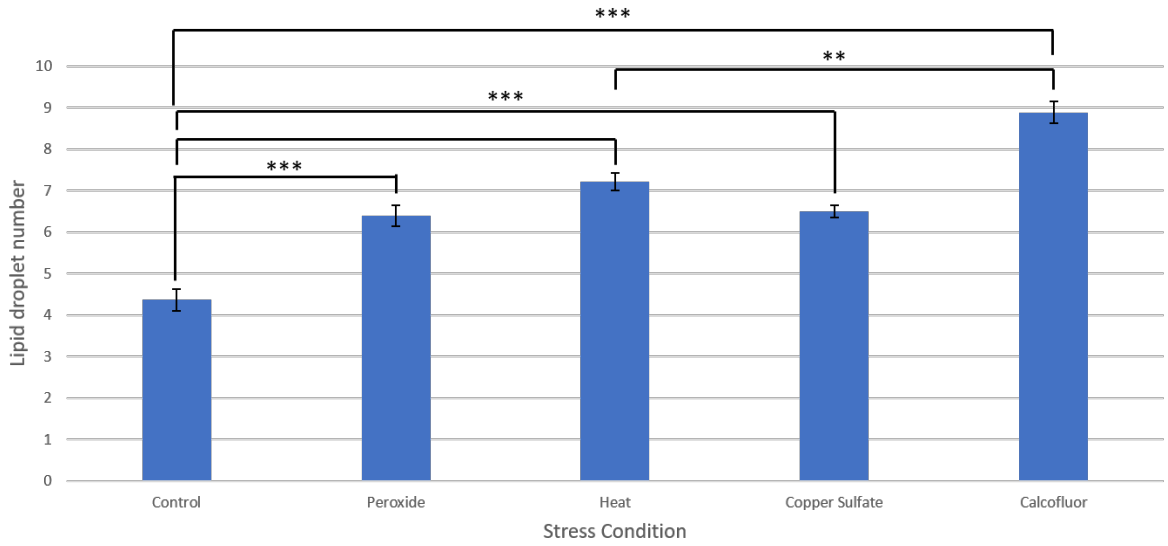

Figure 3.3.2 Quantification of lipid droplets in stressed and unstressed *S. cerevisiae* cofilin 1-5 wild type cells were grown overnight in YPD, and then inoculated to an OD_{600} of 0.1. Cells were then allowed to grow for 24 hours, aliquoted into equal amounts, and treated to a variety of stresses. LD540 staining allowed for the visualisation of lipid droplets within the cell. For each condition, the number of lipid droplets were hand-counted in 150 cells, and this was done in triplicate. The average lipid droplet number from each replicate. One-way ANOVA test was performed. (*- P<0.05, **- P<0.01, ***- P<0.001)

As can be seen in figure 3.3.2, the average number of lipid droplets per cell when unstressed was four. These lipid droplets could generally be seen surrounding the vacuole, perhaps indicative of their propensity to undergo lipophagy. Each of the stresses increased the number of lipid droplets present within cells, with calcofluor treatment eliciting the strongest

effect, with approximately double the amount of lipid droplets visible within cells (Figure 3.3.3). Calcofluor white is a dye that binds to chitin within the fungal cell wall; in doing so, in doing so, it exudes a cell wall stress that triggers action of the CWI pathway[111]. This observation led us to believe that lipid droplets were in some way linked to cell wall stress signalling. Representative cells from each condition are shown in figure 3.3.3.

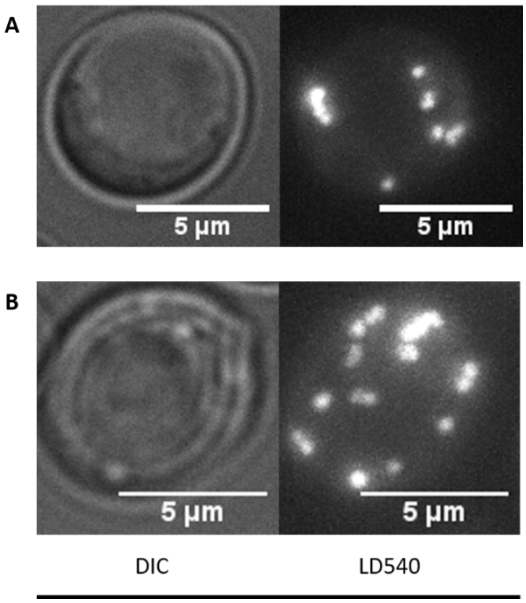

Figure 3.3.3 Lipid droplets in wild type cells with and without calcofluor treatment Images that best represent the populations observed when wild type cells are stained with LD540 in **(A)** wild type cells following 26 hours' total growth and **(B)** wild type cells grown for 24 hours, then subjected to a 100µM calcofluor stress for two hours.

Because of the apparent change in lipid droplet configuration upon calcofluor treatment, it was necessary to observe the effects of these stresses on the localisation of a variety of the components of the CWI pathway. In order to observe the effects of cell wall integrity stress on Pkc1p localisation, a plasmid expressing GFP tagged PKC1, was transformed into the wild type and cofilin 1-5 background strains. These backgrounds were then grown to stationery phase under standard conditions and subjected to a 2 hour calcofluor stress, then observed using fluorescence microscopy (Figure 3.3.4).

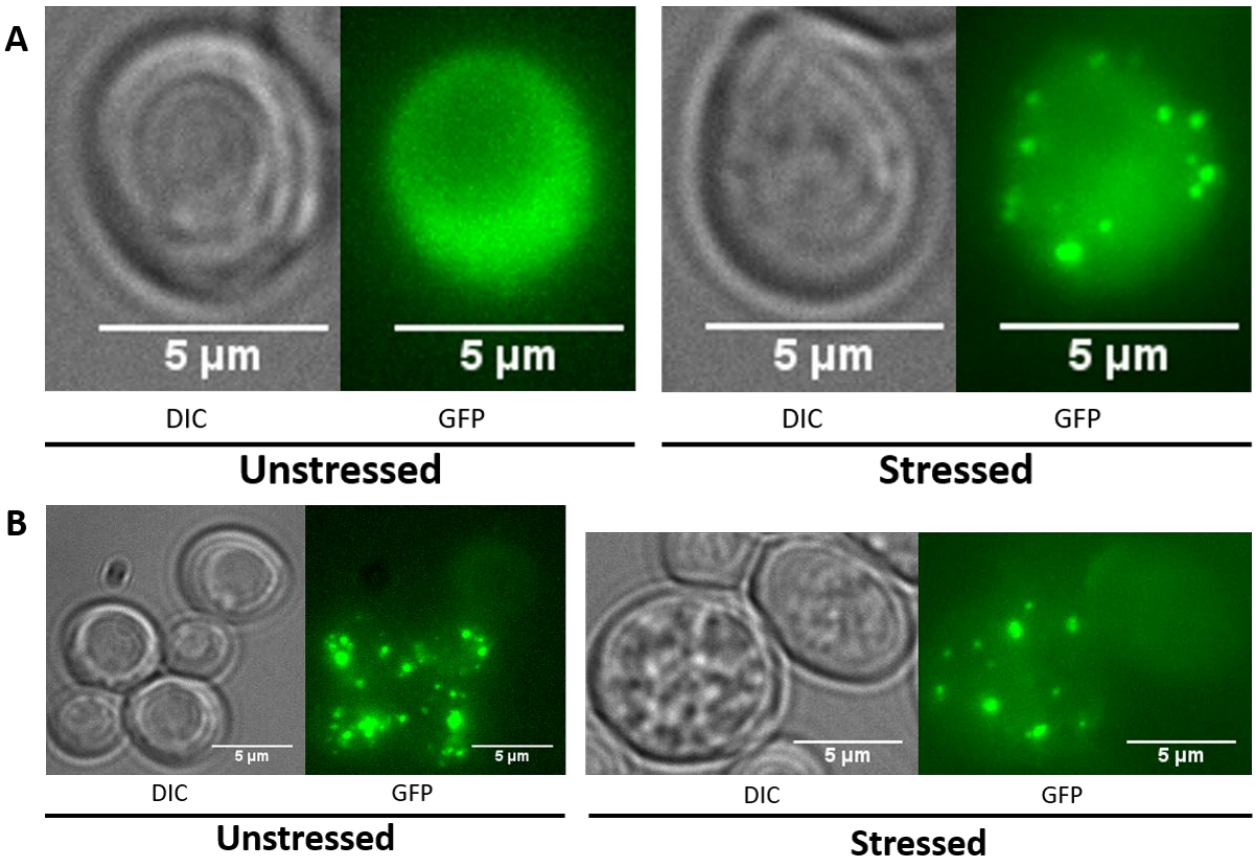

Figure 3.3.4 Pkc1p forms foci during times of stress Fluorescence microscopy of both wild type and cofilin 1-5 mutant cells transformed with a PKC1-GFP plasmid **(A)** representative images of both unstressed and stressed wild type cells and their Pkc1p localisations during stationary phase **(B)** representative images of unstressed and stressed cofilin 1-5 cells with Pkc1p-GFP during stationary phase. Stressed cells received a 100µM calcofluor stress for 2 hours before observation.

In wild type cells PKC1-GFP was dispersed through the cytoplasm. However, following a 2 h calcofluor stress, a significant proportion of cells displayed GFP foci within the cytoplasm (Fig 3.3.4A). In contrast PKC1-GFP foci were visible within cof1-5 cells before and after application of stress (figure 3.3.4B). The next component of the CWI MAPK pathway observed within the wild type and cofilin 1-5 backgrounds was the terminal MAPK in the CWI pathway, Slt2p. In

order to observe the effects of cell wall integrity stress on SLT2 localisation, a plasmid construct expressing GFP tagged Slt2p, was transformed into both the wild type and cofilin 1-5 background strains. These strains were subjected to the same calcoflour stress and observed by fluorescence microscopy (Figure 3.3.5).

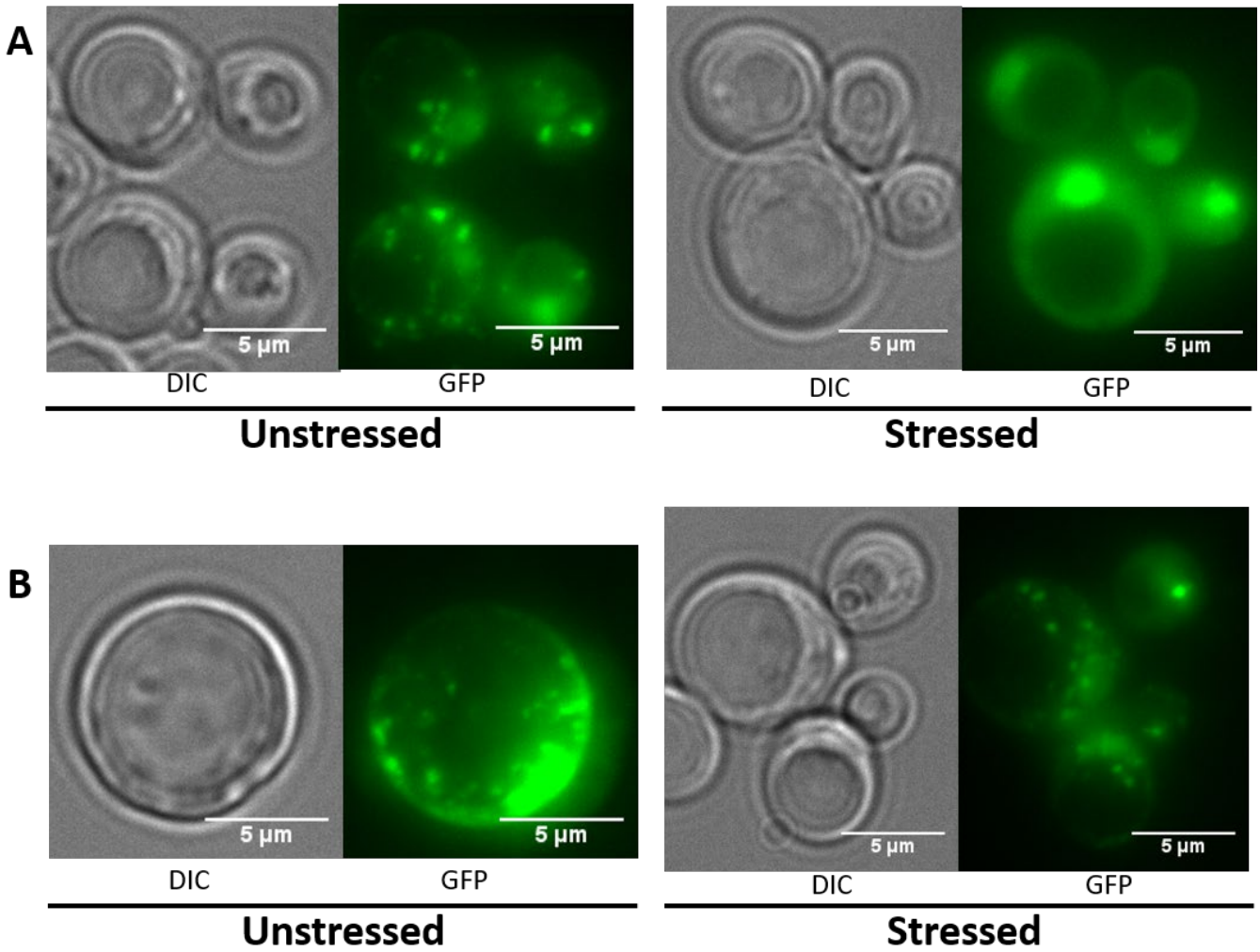

Figure 3.3.5 Slt2p localises to the nucleus in wt *S. cerevisiae* upon CWI activation in wild type cells Both the wild type and cofilin 1-5 backgrounds containing Slt2p-GFP tags were grown overnight in a rich YPD growth medium under standard growth conditions, and then inoculated to an OD_{600} of 0.1 and grown for 24 hours, and subsequently observed with fluorescence microscopy with and without a 2 hour calcofluor treatment **(A)** Representative images of wild type Slt2p-GFP **(B)** Representative images of Cofilin 1-5 Slt2-GFP

In the unstressed wild type, the Slt2p-GFP signal was generally seen to be dispersed throughout the cell; a number of foci and a general cytoplasmic fluorescence is seen, though a number of the population displays a nuclear localisation. Upon calcofluor treatment, the vast majority of wild type cells exhibit a nuclear Slt2p-GFP signal, indicative of its capability to translocate into the nucleus to activate various downstream transcription factors, although the proportions of cells eliciting nuclear localisation is yet to be fully quantified. In the cofilin 1-5 background, treatment of the cells with calcofluor made seemingly no difference; there was a general split population, some exhibiting strong nuclear localization and others displaying prominent cytoplasmic foci. These data suggest that wild type and cof1-5 cells exhibit different localisation of Pkc and slt2 that support our observations that cof1-5 cells exhibit altered CWI signalling activity.

3.4 Analysis of *Dga1Δ* and *Lro1Δ* by fluorescence microscopy

Given that a number of phenotypes observed in cof1-5 cells appear to attributable to CWI signalling activity and that one of these, flocculation, appeared to be reduced upon *DGA1* or *LRO1* deletion, we performed further morphological analyses. Both light microscopy fluorescent microscopy were conducted to observe the effects of *DGA1* or *LRO1* deletion upon cell size or lipid droplets number.

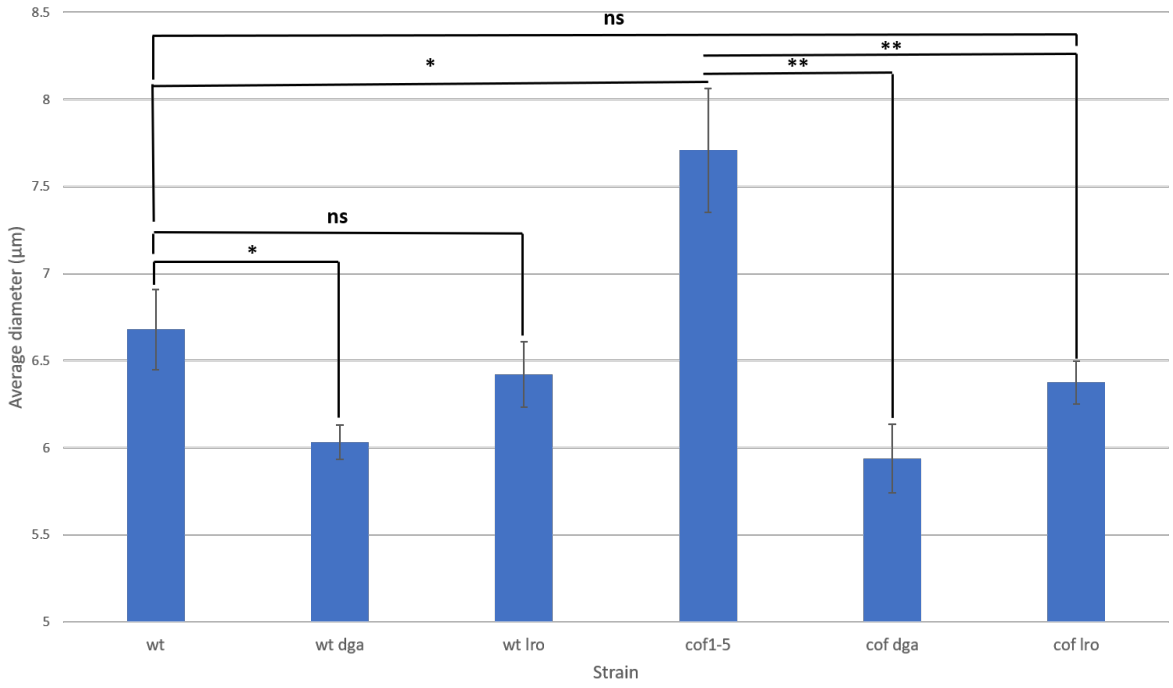

Figure 3.4.1 Deletion of *DGA1* and *LRO1* affect mother cell diameter in both wild type and cofilin 1-5 *DGA1* and *LRO1* deletion strains in both wild type and cofilin 1-5 backgrounds were grown overnight in selective media under standard growth conditions, inoculated to an OD_{600} of 0.1 and allowed to grow for a further 24 hours. Following microscopy, 150 cells diameters were measured in biological triplicate for each strain. One-way ANOVA test was performed. (*- P<0.05, **- P<0.01, ***- P<0.001)

A series of microscopic images were taken and from these the diameters of cells were measured using Image J. Cells expressing the cof1-5 allele were significantly larger than the wild type, with a mean diameter of approximately 8µm compared to 6.5µm (Fig 3.4.1). However deletion of *LRO1* or *DGA1* led to a significant reduction in diameter of the cofilin1-5 cells (Figure 3.4.1) . Deletion of *DGA1* also led to a reduction in the size of wild type cells, this

was not observed upon deletion of *LRO1*. The functions of both *DGA1* and *LRO1* would therefore appear to be important in developing the large cell size observed in cof1-5 cells.

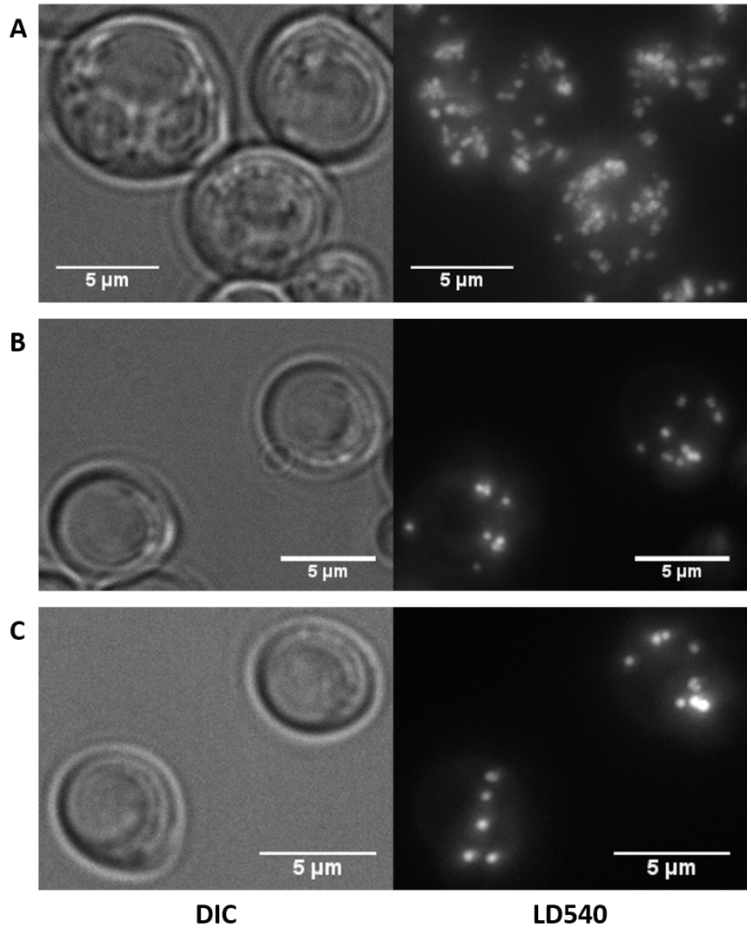

Figure 3.4.2 Deleting *DGA1* and LRO reduces LD540 foci in cofilin 1-5 background *Cof 1-5* background strains were grown in YPD containing 200µM G418, and subsequently inoculated to an OD_{600} of 0.1 and allowed to grow for 24 h. Following LD540 staining, lipid droplets were observed. **(A)** DIC and LD540 images of the cofilin 1-5 strain **(B)** the cofilin 1-5 dga*1Δ* strain **(C)** images taken of the cofilin 1-5 *lro1Δ*

LD540 staining of the *cof 1-5*parental strain, alongside *cof1-5 dga1ΔI and cof1-5 lro1Δ* reveal a reduction in the quantity of visible lipid droplets within the cells (figure 3.4.2). Although this

effect was readily apparent by eye and reproducible, the numbers of lipid droplets in these strains has not as yet been quantified and will be an important extension of this work.

3.5 Assessment of necrosis in wild type, *cof1-5*, *cof1-5 dga1Δ* and *cof1-5 lro1Δ* cells using flow cytometry

We have observed that the hyper-activation of CWI signalling associated with cof1-5 cells results in an increase in the necrotic population found within a stationary phase culture (Dr. Patrick Rockenfeller, Unpublished observations). We sought to determine whether the formation of excessive lipid droplets may contribute to this phenotype using flow cytometry. To determine the overall viability and necrosis we determined the percentage of cells that would take up propidium iodide, which marks necrosis, and which were capable of forming a colony, using a colony forming assay.

Cells were allowed to grow to stationary phase before analysis. The only cells that may be stained with PI are those with a compromised plasma membrane, such as the cells which have undergone necrosis. Flow cytometry provides a means to separate the two populations, unstained and stained, to determine the proportion of cells that have undergone necrosis at a given time point. The first experiment to be conducted was the classification of necrotic populations in both the wild type and cofilin 1-5 cell populations. At 22 h, each background was treated to either 200µM calcofluor stress, 100µM of the antifungal drug, cercosporamide (which acts as a Pkc1p inhibitor and thus a CWI inhibitor), or a combination of the two. The levels of necrosis were recorded after both 24 and 48 hours (figure 3.5.1).

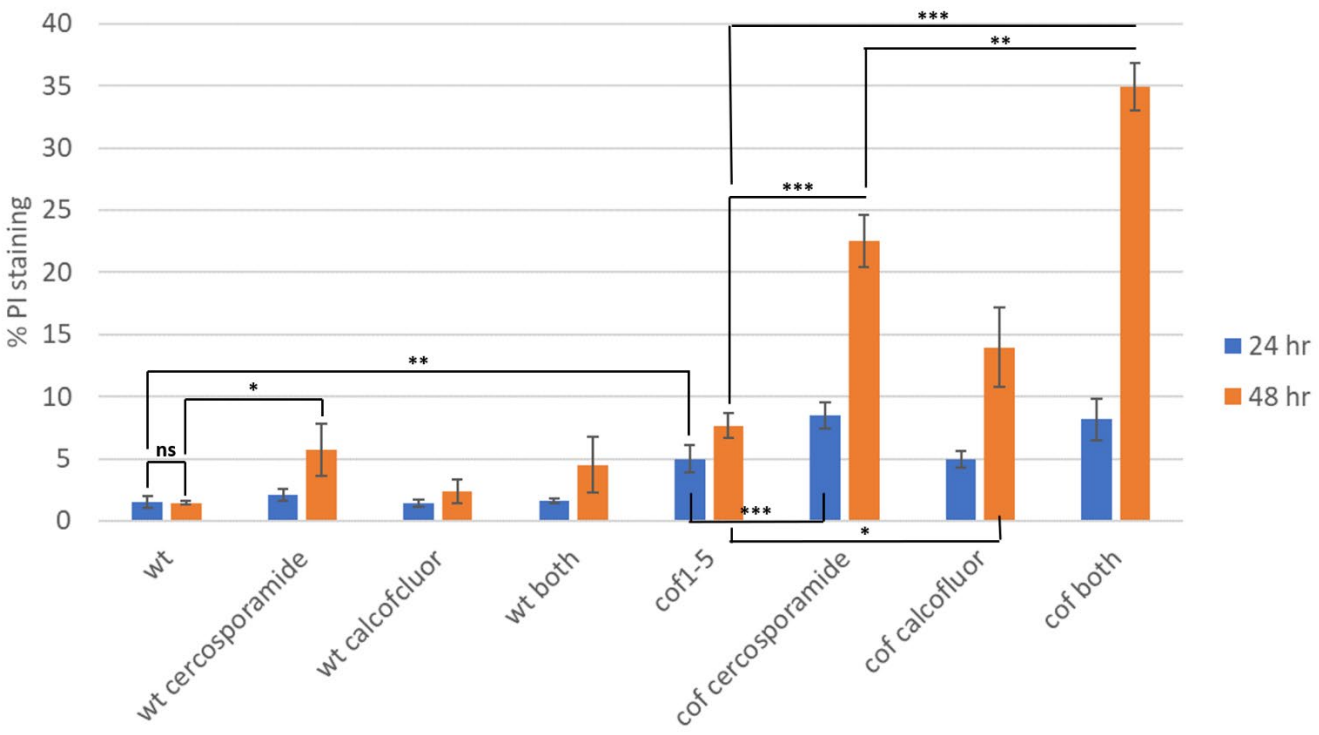

Figure 3.5.1 Pkc1p inhibition of cofilin 1-5 heightens necrosis at 24 and 48 hours wild type and *cof1-5* were grown overnight and inoculated to an OD_{600} of 0.1, then grown at 30°C. After 22 h growth, cells were subjected to either 100µM cercosporamide, 200µM calcofluor or both, and allowed to grow for a further 2 h. At 24 h growth, 30µL of each condition was harvested and stained with 4µg/mL propidium iodide, and the necrosis quantified by flow cytometry. The remaining cell culture was allowed to grow for an additional 24 h, in the same media with no additional drug or calcofluor added, before a second processing of the samples. Experiment performed in triplicate. One-way ANOVA test was performed. (*- P<0.05, **- P<0.01, ***- P<0.001)

In the wild type cell population, Pkc1 inhibition by cercosporamide showed no significant change in PI staining after 24 h, but there was a significant difference in PI% necrotic cells upon cercosporamide treatment at the 48 h timepoint. Calcofluor treatment of wild type

cells had no significant effect upon necrosis after 24 h or 48 h. A combination of cercosporamide and calcofluor treatment displayed no increase in necrosis at the 24 or 48 h timepoints. Given that at 48 h, cersporamide treatment alone increased necrosis, it may be that the presence of calcofluor in the combination treatment rescued this necrosis.

Cells expressing the *cof1-5* allele displayed a higher level of necrosis when compared to the wild type. At 24 hours, approximately 5% of the population was necrotic and this rose to 7.5% at 48 h. Cercosporamide treatment had a more profound effect on cof1-5 cells than it had on wild type with over 20% of the population being necrotic after 48h. When treated with calcofluor, much like the wild type, there was no apparent effect on necrosis after 24 hours, but this did increase after 48h. Concurrent treatment with both cell wall stress and inhibition of the CWI pathway in the cofilin 1-5 background led to the largest increase, with approximately one third of the population being necrotic at 48 h (fig 3.5.1).

Following this we sought to discern whether *DGA1* or *LRO1* played a role in the regulation of necrosis within the wild type and cofilin 1-5 backgrounds (fig 3.5.2).

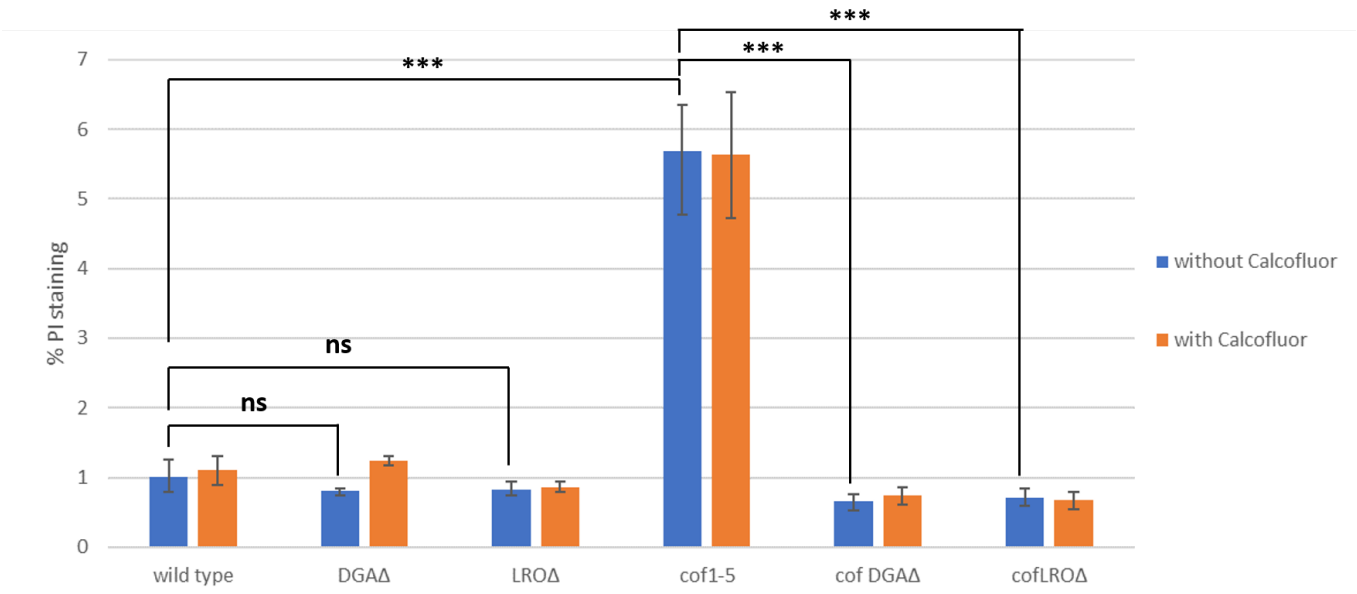

Figure 3.5.2 DGA and LRO deletion rescues the necrosis associated with the cof1-5 mutation

overnight and inoculated to an OD_{600} of 0.1, then allowed to grow for 24 hours total. PI staining and FACS analysis were then performed and the % of necrotic cells calculated. One-way ANOVA analysis was performed. (***- P<0.001)

As seen in previous experiments, the cofilin 1-5 background displayed a higher proportion of necrotic cells at 24 hours when compared to the wild type. PI analysis of the *DGA1* and *LRO1* deletion strains revealed a significant decrease in the necrosis associated with cofilin 1-5 at 24 h, aligning them with a necrotic population comparable to that of the wild type strains. Deletion of *DGA1* and *LRO1* in the wild type has seemingly no effect on the levels of necrosis at 24 hours. These data suggest a direct role for the regulation of lipid metabolism in the control of necrosis. No significant difference may be seen with and without calcofluor stress in deletion strains at 24 h. It would be necessary to repeat the experiment with a 48 h

timepoint to investigate further whether the deletions would have an impact on the cell's response to CWI stress.

3.6 CFU assays to assess viability for parental and deletion strains in both backgrounds

When using a technique such as PI staining, it is necessary to corroborate results with a clonogenic assay such as a CFU assay to observe viability.Therefore the aforementioned flow cytometry experiments to assess necrosis were run concurrently with colony forming unit assays to assess viability. The first was the cercosporamide experiment (figure 3.6.1)

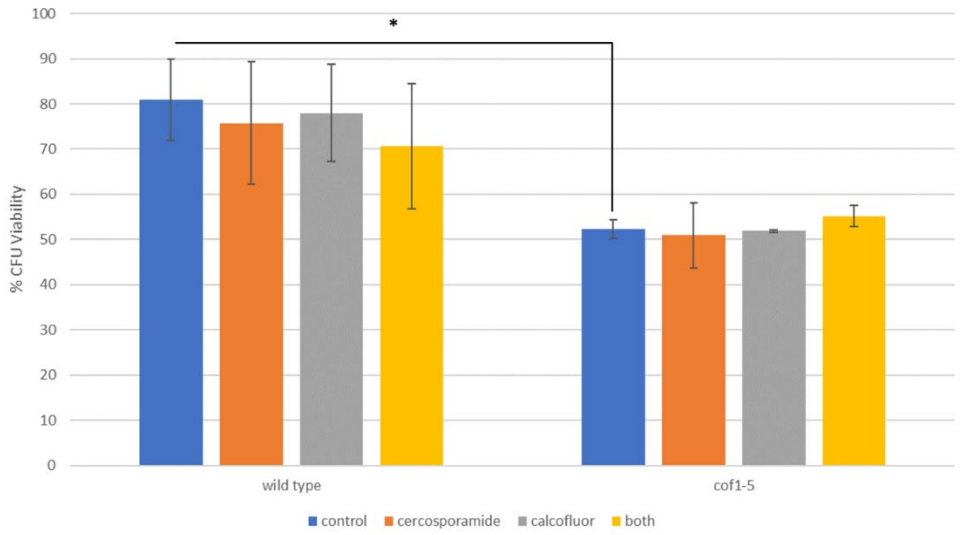

Figure 3.6.1 Viability of wild type and cofilin 1-5 cells upon cells wall stress Wild type and *cof1-5* were grown overnight and inoculated to an OD_{600} of 0.1, then grown at 30°C. After 22 h growth, cells were subjected to either 100µM cercosporamide, 200µM calcofluor or both, and allowed to grow for a further 2 h. At 24 h growth, ~250 cells were plated on YPD per sample and allowed to grow at 30°C for 48 hours. The percentage of plated cells which were

are able to form a colony (colony forming unit, or CFU) is shown. Experiment was completed in triplicate. One-way ANOVA test was performed. *-P<0.05

Wild type and *cof1-5* cells were treated with 100µM cercosporamide, 200µM calcofluor or both, in the same manner as the FACS experiment displayed prior (fig 3.5.1); 250 cells were plated on YPD at 24 h growth following a 2 h treatment with cercosporamide or calcofluor. These plates were then incubated at 30^{o}C for 48 hours, at which point the number of colony forming units (CFUs) were determined.

In the wild type cells, we observed no discernible difference between untreated controls and cells treated with either cercosporamide or calcoflour (figure 3.6.1).

Cultures formed from cof1-5 cells displayed a reduced viability when compared to wild with an average CFU of 50% in this series of experiments. Suprisingly we observed no significant difference in viability when cells were treated with cercosporamide or calcofluor (figure 3.6.1). This finding conflicts with our finding that treatment of cof1-5 cells with calcoflour or cercosporamide increases necrosis. Although the nature of the assay is such that all plating is approximate, and hence a degree of variability may mean less sensitivity to the minor changes in levels of necrosis we saw with PI staining. It may be necessary to plate cells at the 48 hour timepoint to discern any difference as a result of cercosporamide or calcofluor.

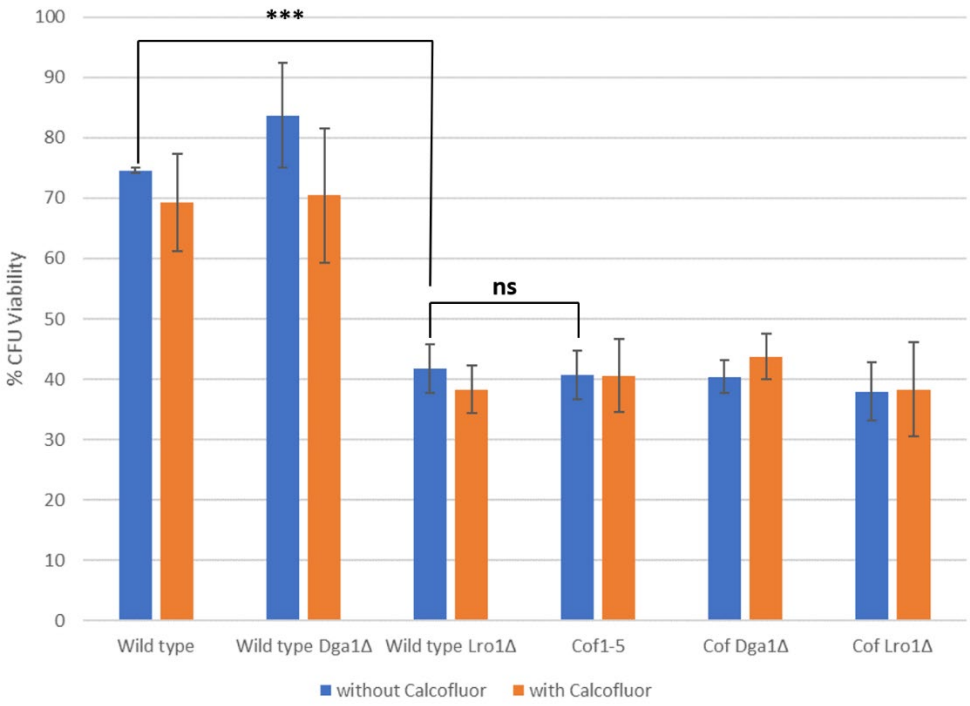

Figure 3.6.2 CFU assay of wild type and *cof1-5 dga1Δ* and lro1Δ when treated with cell wall stress . Parental, *dga1Δ* and *lro1Δ* strains in wild type and *cof1-5* backgrounds were grown overnight, inoculated in YPD to OD_{600} 0.1, and allowed to grow for 24h. At 24 h growth, ~250 cells were plated on YPD per sample and allowed to grow at 30°C for 48 hours. The percentage of plated cells which were are able to form a colony (colony forming unit, or CFU) is shown. Experiment was completed in triplicate. One-way ANOVA test was performed. ***-P<0.001

CFU assays were performed using the *DGA1* and *LRO1* deletions in the wild type and cofilin 1-5 mutant background. As before, 250 cells were plated on YPD agar and allowed to grow for 48 hours. Each strain was also subjected to a 2 hour calcofluor stress. Again, there was no discernible effect on the viability of cofilin 1-5 upon deletion of *DGA1* and *LRO1*. This finding is also in contrast to our finding that there was a difference in PI staining in these strains,

however the standard deviation observed in my CFU assays may mean these relatively small differences were not detectable by CFU assay. In the wild type background, this series of experiments displays approximately 75% of the population to be viable. There was no apparent effect of calcofluor stress on viability in this instance (figure 3.6.2). Deletion of *DGA1* had no significant effect on the overall viability of the wild type. LRO deletion, on the other hand, significantly reduced viability of wild type cultures, down to a level comparable to that of the cofilin 1-5 background.

3.7 Western blot analysis to determine the role of lipid droplets in CWI activation

Having seen a loss of necrosis, flocculation and lipid droplet accumulation within *cof1-5* upon deletion of *DGA1* and *LRO1*, Western blot analysis was conducted to ascertain whether these deletions had rescued from these phenotypes by deactivating the constitutive CWI signalling.

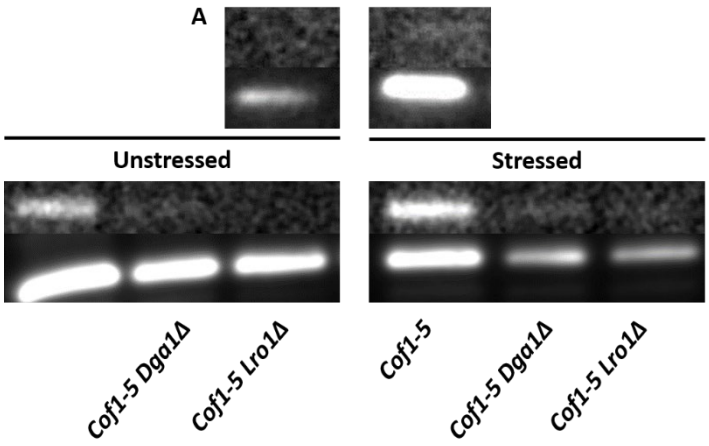

Figure 3.7.1 Phospho-Slt2 detection through Western blot analysis Wild type cells, *cof1-5* and *cof1-5 dga1Δ and cof1-5 lro1Δ* were grown in YPD and were allowed to grow to stationary phase prior to extraction. The application of a calcofluor stress to each strain was used as a

positive control to display CWI pathway activation in the wild type under stress. Blots were probed for phosphorylated Slt2p to confirm CWI activation, stripped, and then reprobed for Act1 in order to ensure uniform protein sample loading.

As previously explained, the CWI branch of MAPK signalling is an instigator of numerous stress responses as a result of external cell wall stress. A signalling cascade beginning with PKC1 and ending with SLT2 phosphorylation coordinates transcriptional regulation in order to elicit these responses. As such, western blot analysis was performed on the wild type and all mutants in *cof1-5* background. Wild type deletion strains were omitted due to temporal constraints and technical issues.

Each strain was allowed to grow to stationary phase. Unstressed and stressed versions of wild type, *cof1-5* and *cof1-5 dga1Δ and cof1-5 lro1Δ* were then subjected to protein extraction and Western blot analysis to detect phospho-Slt2 with an antibody that specifically binds phosphorylated Slt2. Following the detection of Slt2, each blot was then stripped to remove all antibodies, and then retreated with another series of antibodies to detect actin, a protein which was often used as a loading control in Western blotting. This acts to ensure similar amounts of protein have been loaded, and as such it can be certain that observed levels of SLT2 are comparable.

In the wild type, little to no phosphorylated SLT2 was detected whilst unstressed during stationary phase, suggesting that the CWI signalling pathway is inactive. A faint band was visible when cells were stressed with calcofluor, indicative of a degree of CWI pathway activation. In contrast, in the cofilin 1-5 background, there was a prominent phosphor-Slt2

band in both the unstressed and stressed cells (Figure 3.7.1) suggesting constitutive pathway activation.

In both wild type and cof1-5 backgrounds, deletion of *DGA1* and *LRO1* had prominent effect on the level of SLT2 phosphorylation that could be detected. Despite similar levels of protein loading, as displayed by the actin loading control, the bright band associated with the cofilin 1-5 band was greatly diminished. We were also unable to detect a strong phospho-slt2 band upon cell wall stress in wild type cells (figure 3.7.1), which could be the result of a technical issue, and further investigation will be important to the future of this study. Although the mechanism remains uncertain, the blotting analysis reveals that DGA and LRO deletions, and hence disruption of TAG production and lipid droplet formation, in some way reduces *S. cerevisiae*'s ability to activate the CWI branch of MAPK signalling.

Chapter 4

Discussion

Lipid droplets are lipid storage vesicles that are highly conserved throughout higher eukaryotes. They are formed of a neutral lipid core and encased within a phospholipid monolayer embedded with protein. The presence of LD's is often regarded as a means to sequester excess FFAs to buffer against lipotoxicity, and to ensure availability of phospholipid precursors should the need arise[10,32,132]. However it has even been speculated that their presence within the cell may act as a first form of defence against ROS production and as a platform for signalling events within the cell[12,140,144]. The conversion of FFAs into the neutral lipid components (TAG and SE) of a lipid droplet is primarily controlled by four enzymes, namely Dga1p, Lro1p, Are1p and Are2p, the first two of which have been focussed on in this study.

Here, we sought to elucidate the impact of lipid droplets on intracellular stress responses in *Saccharomyces cerevisiae.* Previous works have shown the accumulation of lipid droplets under stress[92] and suggested this to be both protective and destructive to the cell. Previous work within the Gourlay lab led us to hypothesise a link between lipid droplet formation and the CWI branch of MAPK signalling. This is highlighted by the number of lipid droplets present within the *cof1-5* mutant background, a strain which exhibits constitutive CWI signalling (unpublished data).

To test the hypothesis that LD formation and CWI signalling were linked, I examined their formation in response to the application of cell wall stress. The application of agents known to impart cell wall stress was sufficient induce LD formation. This was most notable under calcofluor white stress which led to a two fold increase in LD formation. These experiments

suggest a correlation between the application of exogenous stress and LD number and the findings are in line with previous published observations that link LD formation to stress.

It has been established in previous studies that overexpression of *DGA1* increases CLS[12], and in some instances, loss of lipid droplets leads to a loss of drug resistance[27]. There is therefore some published evidence to suggest that LD formation can modulate stress response in yeast cells. To investigate whether the increase in LD formation was involved in modulating CWI pathway activity we deleted key components in the TAG synthesis pathway to impair the cells ability to produce LD's. Specifically we generated *dga1Δ* and *lro1Δ strains* in both the wild type and *cof1-5* mutant background. The effect of doing so is a reduction in TAG content of LDs[25] that may be compensated for somewhat by an increase in SE content[36], but with a general reduction in LD formation[10].

The experiments revealed that loss of either *DGA1* or *LRO1* in the *cof1-5* background significantly reduced flocculation, a strong indicator of CWI activity. This effect could be observed within growth curves and within the culture itself as in both cases deletion of *DGA1* and *LRO1* led to growth curves that appeared similar to wild type. Deletion of *LRO1* in the wild type led to a significantly slower growth rate when compared to the parental strain. This could be attributable to a reduction in the cell's ability to store oleic acid as TAG[9]. We hypothesised that deletion of *LRO1* or *DGA1* led to a reduction in CWI signalling and subsequent loss of flocculation observed in the *cof1-5* background. Given the control that CWI signalling has over growth and cell cycle progression[89,99,100], the slower growth in wild type *lro1Δ* might indicate a reduced capacity for the cell to activate the CWI pathway.

The idea that *DGA1* and *LRO1* can impact upon the CWI pathway in *cof1-5* cells was bolstered by results gained from PI staining. The wild type parental strain population contained less than 1% necrotic cells after 24 h growth, and the wild type *dga1Δ* and *lro1Δ* were comparable to this. However, cof1-5 cultures contained a significantly higher proportion of PI positive, or necrotic, cells that was to that of the wild type upon deletion of *DGA1* or *LRO1.* This finding may also suggest that deletion of *DGA1* and *LRO1* had the effect of reducing CWI signalling as inappropriate cell wall synthesis may impair cell viability. Further confirmation of our hypothesis came through Western blot analysis; the prominent phospho-Slt2p banding seen within the cof1-5 parental strain is indicative of constitutive CWI pathway activation. Phospho-Slt2p was greatly reduced upon deletion of *DGA1* or *LRO1* suggesting a role for lipid droplets. The application of calcoflour stress to wild type cells led to a detectable, but faint phospho-Slt2p band. Whether this highlights that cof1-5 cells experience higher levels of Slt2p phosphorylation is unclear as we did not have an antibody specific to the non-phosphorylated form of Slt2p. These experiments will require repetition to control for total Slt2 levels using an epitope tagged version, or generation of an anti-Slt2p antibody.

We were also able to confirm CWI activation through the use of the Pkc1 inhibitor cercosporamide. Treatment of wild type cells with cercosporamide led to a significant increase in necrosis compared to that of the control condition, indicating the key role this pathway plays in cell integrity. The levels of necrosis were also significantly increased in *cof1-5,* indicating that a functional CWI pathway is present in this background. However, the increases observed were larger than those in wild type cells, perhaps as *cof1-5* cells have impaired cell walls to begin with. This was verified by co-treatment of cells with both

calcoflour and cercosporamide at the same time. Treatment of *cof1-5* with calcofluor showed no discernible effect at the 24 hour following a 2 hour stress, but could be seen to elevate by 48h. The addition of both calcofluor and cercosporamide treatment had the effect of greatly increasing the necrotic population at 48 hours in the *cof1-5* mutant, though displayed no distinguishable effect from the control in wild type cells. It is likely that these findings reflect that a balance between cell wall structure and CWI pathway activity is essential to ensure cell viability under conditions of cell wall stress. Such a balance is present in wild type cells but has been lost in *cof1-5* cells.

Viability was assessed in wild type, *cof1-5, Δdga1, Δlro1, cof1-5 Δdga1* and *cof1-5Δlro1* strains under conditions of cell wall stress and CWI and Pkc1 inhibition . While there was an obvious difference in viability between the wild type and the cof1-5 mutants I did not detect further changes upon calcofluor or cercosporamide stress. This could be a result of the level of variability obtained when using the CFU assay, however at this stage it is not clear as results obtained using PI staining methods and CFU assays did not align well.

Interestingly we did not observe changes in viability within the *cof1-5* culture upon deletion of *DGA1* or *LRO1* despite their apparent loss of constitutive CWI signalling, flocculation and PI staining. It may be that cof1-5 PI positive cells result from altered cell wall and membrane structure that permits PI uptake, but which has not led to cell death. Alternatively these findings may reflect a technical issue such that the PI staining data does not reflect a dead cell population, or indeed that the CFU protocol variability has led to spurious findings. In order to be certain, it is necessary to corroborate the PI staining observations with another quantitative measure of viability. Given the greater proportion of PI stained cells in both wild

type and *cof1-5* after 48 hours, performing CFUs and plating cells at the same timepoint as this may make any differences between those with and without Pkc1 inhibition or calcofluor treatment. It may therefore be necessary to corroborate the PI data depiction of viability with another assay, such as timelapse photomicroscopy with phloxine B. The assay utilises a dye that permeate cells, but is actively pumped out of cells that are metabolically active. Calculating the proportion of stained cells with and without cercosporamide treatment, therefore, may provide a clearer picture of the action of the CWI integrity pathway[145]. Considering that according to these results *cof1-5* displays a 5% PI stained population at 24 hours, and an overall viability of 40-50% from CFU data, the vitality of the population should also be taken into account. A cell's vitality refers to it's ability to divide. A cell may be unable to divide, but not be dead. Further experimentation would be required to fully categorise the viability and vitality of populations grown from these strains. The use of the FUN-1 stain could elucidate the cell vitality of these populations; in dead or metabolically inactive cells, FUN-1 fluoresces green within the cytoplasm; a metabolically active cell is capable of processing the stain, and a red probe may be seen within the vacuole[145,146]. Running this alongside an enzymatic assay, such as the Cell Counting Kit-8, may provide useful insights into the metabolic capabilities of *cof1-5* and the deletion strains.

After establishing a link between LDs and CWI signalling, the main question to be addressed is the nature of the relationship between the two. *Cof1-5* displays both constitutive CWI signalling and excessive proliferation of LDs. Activation of CWI signalling begins with an exogenous stress, inducing guanine nucleotide exchange of Rho1 by its GEFs, Rom1 and Rom2[93,95]. Rho1 is a Ras-like GTPase that, when activated, directly activates Pkc1 and thus

the CWI pathway[102] Rho1 has also been described as a component of the GS complex required for cell wall synthesis[106,107]. It may be that the proliferation of LDs in *cof1-5* impact upon the structure of the plasma membrane due to insufficient available precursors for phospholipid metabolism, or that the plasma membrane suffers as a result of dysregulated actin. Either of these scenarios could lead to activation of CWI signalling by applying a stretch to the Wsc1 mechanosensor within the plasma membrane, which interacts with Rom2 and causes activation of Rho1[95]. CWI signalling is thought to be controlled by a negative feedback loop (a MAPK dependant feedback mechanism) which may be ineffective with the cell's polarised actin, giving rise to constitutive CWI signalling. Deletion of *ROM2* in the wild type and *cof1-5* backgrounds would need to be generated in order to pursue this further.

It should considered that the elevated LD content seen in *cof1-5* would likely cause a sequestration of intracellular DAG as neutral TAG within LDs[10]. DAG has been attributed to facilitating the fusion of vacuole[147], and thus it may be that the fragmented vacuole seen in *cof1-5* may be partially attributed to the absence of DAG. This reduction in DAG content may also impair the structure of the cell wall, given that DAG is required for biosynthesis of GPI proteins[84,86,87]. Deletion of *DGA1* and *LRO1* may indeed alleviate this effect by increasing available intracellular DAG to facilitate vacuolar fusion and loss of abhorrent CWI signalling.

There is also the possibility that mutated cofilin may cause abhorrent signalling through redistribution of PIP_2. Non-mutated cofilin has a large PIP_2 binding site, as PIP_2 is necessary for cofilin inhibition[148–150].The introduction of the *cof1-5* mutation may reduce PIP_2's affinity for cofilin binding, leading to a redistribution. PIP_2 is necessary for the correct localisation of Rom2 for the activation of Rho1[103], and so the redistribution of PIP_2 with mutated cofilin may attribute to the abhorrent CWI signalling seen in *cof1-5.* It would therefore be worthwhile to

observe the localisations of PIP_2 in these strains and determine whether the impact of deleting *ROM2, DGA1* and *LRO1.*

It is also possible that lipid droplets may be acting as a signalling platform for the CWI pathway. Fluorescence microscopy was performed in this study to observe the behaviour of slt2p and pkc1p within both backgrounds while the cells are under cell wall stress. In unstressed wild type cells we observed a disperse pkc1p GFP signal, with the addition of calcofluor causing more of these cells to display intracellular foci. The same could be seen in some of the wild type with an slt2p GFP tag, although most stressed slt2p cells predominantly exhibited a nuclear localisation of the GFP signal, indicative of its role as a regulator of downstream transcription factors. It is possible that the presence of these foci during times of stress may corroborate with the position of lipid droplets within the cell, although this proved difficult to ascertain as the concentration of LD540 required to successfully stain lipid droplets led to an issue in confidently gating LD540 signals from GFP signals with the filters at our disposal. It would also be necessary to observe the behaviour of these CWI signalling kinases within the deletion strains, as if there is physical interaction between the CWI pathway and LDs, it may be that deletion of *DGA1* or *LRO1* in some way inhibit this interaction, leading to deactivation of the pathway. Further microscopy and colocalization studies would be required to determine whether lipid droplets are physically interacting with the CWI pathway.

Future Work

- It is necessary to properly establish whether the foci seen in the GFP tagged pkc1p or slt2p are in any way interacting with lipid droplets within the cell. It would be necessary to use microscopy software with the potential to gate the GFP and LD540 derived signals to ensure there was no bleed-through and false positive results. Similar to this, the transformation of the Pkc1-GFP and Slt2-GFP plasmids into the deletion strains would be able to elucidate whether these deletions somehow disrupt interaction between CWI signalling components and LDs.
- Primers were designed for to delete *ARE1* and *ARE2*. It would be interesting to perform these transformations in both the wild type and cofilin 1-5 backgrounds, to see if disruption of SE lipid droplet content has the same effect of reduced CWI signalling, or if that effect is exclusive to TAG disruption. Such a finding may be necessary to decipher how the disruption of signalling occurs.
- The deletion strains should be subjected to cercosporamide treatment in the same manner as their parental cells were. It may be revealed that these strains are unable to decide upon regulated cell death due to the loss of CWI signalling capabilities, and thus potentially a larger population would become senescent in this instance.
- The effect of the *DGA1 and LRO1* deletions on growth and progression toward stationary phase should be further explored. It may be interesting to do more growth curve analyses with these strains in the presence of varying concentrations of calcofluor stress, for example.
- Determining the impact of *cof1-5* on CWI signalling, and thus how deletion of TAG regulating enzymes inhibits this signalling, may require investigation into the

behaviour of Rho1 and Rom2, and so transformation of Rho1 and Rom2 plasmids into these strains could prove interesting. Rho1 should also be observed within wild type and *cof1-5* backgrounds with deleted Rom2, to determine whether this disrupts constitutive CWI signalling and to better understand the behaviour of lipid droplets in the presence of CWI signalling. Primers have been designed, and further experimentation of *Rom2Δ* in wild type and *cof1-5* mutant strains may reveal more on the nature of the abhorrent CWI signalling within cofilin 1-5.

- The discrepancy in cell diameter observed through microscopy in TAG deletion strains should not be ignored. Unpublished work from the lab has shown that deletion of *POR1 (*a gene that encodes for the mitochondrial outer membrane anion channel) in cofilin 1-5 displays the same deactivation of CWI signalling, as well as rescue from flocculation and vacuolar fragmentation. This link to mitochondria and similarity between the different rescues leads me to wonder whether the smaller, petite cells observed upon deletion of *DGA1* are the result of perturbed growth, or maybe a mitochondrial dysfunction leading to respiratory defects. Respirometry studies of the strains would elucidate these details.

References

1. Wang, C. W. Lipid droplet dynamics in budding yeast. *Cell. Mol. Life Sci.* **72,** 2677–2695 (2015).

2. Markgraf, D. F. *et al.* An ER protein functionally couples neutral lipid metabolism on lipid droplets to membrane lipid synthesis in the ER. *Cell Rep.* **6,** 44–55 (2014).

3. Sorger, D. & Daum, G. Synthesis of triacylglycerols by the acyl-coenzyme A:diacyl-glycerol acyltransferase Dga1p in lipid particles of the yeast Saccharomyces cerevisiae. *J. Bacteriol.* **184,** 519–524 (2002).

4. Fei, W. *et al.* Fld1p, a functional homologue of human seipin, regulates the size of lipid droplets in yeast. *J. Cell Biol.* **180,** 473–482 (2008).

5. van Zutphen, T. *et al.* Lipid droplet autophagy in the yeast Saccharomyces cerevisiae. *Mol. Biol. Cell* **25,** 290–301 (2014).

6. Fei, W. *et al.* A role for phosphatidic acid in the formation of 'supersized' Lipid droplets. *PLoS Genet.* **7,** (2011).

7. Marr, N., Foglia, J., Terebiznik, M., Athenstaedt, K. & Zaremberg, V. Controlling lipid fluxes at glycerol-3-phosphate acyltransferase step in yeast: Unique contribution of Gat1p to oleic acid-induced lipid particle

formation. *J. Biol. Chem.* **287,** 10251–10264 (2012).

8. Jacquier, N. *et al.* Lipid droplets are functionally connected to the endoplasmic reticulum in Saccharomyces cerevisiae. *J. Cell Sci.* **124,** 2424–2437 (2011).

9. Ayciriex, S. *et al.* YPR139c/LOA1 encodes a novel lysophosphatidic acid acyltransferase associated with lipid droplets and involved in TAG homeostasis. *Mol. Biol. Cell* **23,** 233–246 (2012).

10. Adeyo, O. *et al.* The yeast lipin orthologue Pah1p is important for biogenesis of lipid droplets. *J. Cell Biol.* **192,** 1043–1055 (2011).

11. Wilfling, F. *et al.* Triacylglycerol synthesis enzymes mediate lipid droplet growth by relocalizing from the ER to lipid droplets. *Dev. Cell* **24,** 384–399 (2013).

12. Handee, W. *et al.* An Energy-Independent Pro-longevity Function of Triacylglycerol in Yeast. *PLoS Genet.* **12,** 1–25 (2016).

13. Madeira, J. B. *et al.* TORC1 Inhibition Induces Lipid Droplet Replenishment in Yeast. *Mol. Cell. Biol.* **35,** 737–746 (2015).

14. Thoms, S., Debelyy, M. O., Connerth, M., Daum, G. & Erdmann, R. The putative Saccharomyces cerevisiae hydrolase Ldh1p is localized to lipid droplets. *Eukaryot. Cell* **10,** 770–775 (2011).

15. Rajakumari, S., Grillitsch, K. & Daum, G. Synthesis and turnover of non-polar lipids in yeast. *Prog. Lipid Res.* **47,** 157–171 (2008).

16. Czabany, T. *et al.* Structural and biochemical properties of lipid particles from the yeast Saccharomyces cerevisiae. *J. Biol. Chem.* **283,** 17065–74 (2008).

17. Bartz, R. *et al.* Lipidomics reveals that adiposomes store ether lipids and mediate phospholipid traffic. *J. Lipid Res.* **48,** 837–47 (2007).

18. Choudhary, V., Jacquier, N. & Schneiter, R. The topology of the triacylglycerol synthesizing enzyme Lro1 indicates that neutral lipids can be produced within the luminal compartment of the endoplasmatic reticulum: Implications for the biogenesis of lipid droplets. *Commun. Integr. Biol.* **4,** 781–4 (2011).

19. Wang, C.-W., Miao, Y.-H. & Chang, Y.-S. Control of lipid droplet size in budding yeast requires the collaboration between Fld1 and Ldb16. *J. Cell Sci.* **127,** 1214–1228 (2014).

20. Sturley, S. L. & Hussain, M. M. Lipid droplet formation on opposing sides of the endoplasmic reticulum. *J. Lipid Res.* **53,** 1800–1810 (2012).

21. Zanghellini, J., Wodlei, F. & von Grünberg, H. H. Phospholipid demixing and the birth of a lipid droplet. *J. Theor. Biol.* **264,** 952–961 (2010).

22. Baba, T. *et al.* Phosphatidic acid (PA)-Preferring phospholipase A1 regulates mitochondrial dynamics. *J. Biol. Chem.* **289,** 11497–11511 (2014).

23. Connerth, M. *et al.* Oleate inhibits steryl ester synthesis and causes liposensitivity in yeast. *J. Biol. Chem.* **285,** 26832–26841 (2010).

24. Ferreira, T., Régnacq, M., Alimardani, P., Moreau-Vauzelle, C. & Bergès, T. Lipid dynamics in yeast under haem-induced unsaturated fatty acid and/or sterol depletion. *Biochem. J.* **378,** 899–908 (2004).

25. Oelkers, P., Cromley, D., Padamsee, M., Billheimer, J. T. & Sturley, S. L. The DGA1 gene determines a second triglyceride synthetic pathway in yeast. *J. Biol. Chem.* **277,** 8877–8881 (2002).

26. Spanova, M. *et al.* Effect of lipid particle biogenesis on the subcellular distribution of squalene in the yeast Saccharomyces cerevisiae. *J. Biol. Chem.* **285,** 6127–6133 (2010).

27. Sorger, D., Athenstaedt, K., Hrastnik, C. & Daum, G. A yeast strain lacking lipid particles bears a defect in ergosterol formation. *J. Biol. Chem.* **279,** 31190–31196 (2004).

28. Petschnigg, J. *et al.* Good fat, essential cellular requirements for triacylglycerol synthesis to maintain membrane homeostasis in yeast. *J.*

Biol. Chem. **284,** 30981–30993 (2009).

29. Wang, C.-W. & Lee, S.-C. The ubiquitin-like (UBX)-domain-containing protein Ubx2/Ubxd8 regulates lipid droplet homeostasis. *J. Cell Sci.* **125,** 2930–2939 (2012).

30. Athenstaedt, K., Weys, S., Paltauf, F. & Daum, G. Redundant systems of phosphatidic acid biosynthesis via acylation of glycerol-3-phosphate or dihydroxyacetone phosphate in the yeast Saccharomyces cerevisiae. *J. Bacteriol.* **181,** 1458–63 (1999).

31. Dahlqvist, a *et al.* Phospholipid:diacylglycerol acyltransferase: an enzyme that catalyzes the acyl-CoA-independent formation of triacylglycerol in yeast and plants. *Proc. Natl. Acad. Sci. U. S. A.* **97,** 6487–6492 (2000).

32. O'Hara, L. *et al.* Control of phospholipid synthesis by phosphorylation of the yeast lipin Pah1p/Smp2p Mg2+-dependent phosphatidate phosphatase. *J. Biol. Chem.* **281,** 34537–34548 (2006).

33. Su, W. M., Han, G. S. & Carman, G. M. Cross-talk phosphorylations by protein kinase C and Pho85p-Pho80p protein kinase regulate pah1p phosphatidate phosphatase abundance in saccharomyces cerevisiae. *J. Biol. Chem.* **289,** 18818–18830 (2014).

34. Hsieh, L. S., Su, W. M., Han, G. S. & Carman, G. M. Phosphorylation of

yeast Pah1 phosphatidate phosphatase by casein kinase II regulates its function in lipid metabolism. *J. Biol. Chem.* **291,** 9974–9990 (2016).

35. Fakas, S. *et al.* Phosphatidate phosphatase activity plays key role in protection against fatty acid-induced toxicity in yeast. *J. Biol. Chem.* **286,** 29074–29085 (2011).

36. Han, G. S., Wu, W. I. & Carman, G. M. The Saccharomyces cerevisiae lipin homolog is a Mg2+-dependent phosphatidate phosphatase enzyme. *J. Biol. Chem.* **281,** 9210–9218 (2006).

37. Fei, W. *et al.* A role for phosphatidic acid in the formation of 'supersized' Lipid droplets. *PLoS Genet.* **7,** e1002201 (2011).

38. Rockenfeller, P. *et al.* Fatty acids trigger mitochondrion-dependent necrosis. *Cell Cycle* **9,** 2836–2842 (2010).

39. Ren, J. *et al.* A phosphatidylinositol transfer protein integrates phosphoinositide signaling with lipid droplet metabolism to regulate a developmental program of nutrient stress-induced membrane biogenesis. *Mol. Biol. Cell* **25,** 712–727 (2014).

40. Pineau, L. & Ferreira, T. Lipid-induced ER stress in yeast and ?? cells: Parallel trails to a common fate. *FEMS Yeast Res.* **10,** 1035–1045 (2010).

41. Krahmer, N. *et al.* Phosphatidylcholine synthesis for lipid droplet

expansion is mediated by localized activation of CTP:Phosphocholine cytidylyltransferase. *Cell Metab.* **14,** 504–515 (2011).

42. Boumann, H. A., de Kruijff, B., Heck, A. J. . & de Kroon, A. I. P. . The selective utilization of substrates in vivo by the phosphatidylethanolamine and phosphatidylcholine biosynthetic enzymes Ept1p and Cpt1p in yeast. *FEBS Lett.* **569,** 173–177 (2004).

43. Vance, E. Phospholipid Mitochondria * Synthesis in a Membrane Fraction Associated identified. *J. Biol. Chem.* **265,** 7248–7257 (1990).

44. Zhang, Q. *et al.* Biosynthesis and roles of phospholipids in mitochondrial fusion, division and mitophagy. *Cell. Mol. Life Sci.* **71,** 3767–3778 (2014).

45. Murphy, S., Martin, S. & Parton, R. G. Quantitative analysis of lipid droplet fusion: Inefficient steady state fusion but rapid stimulation by chemical fusogens. *PLoS One* **5,** e15030 (2010).

46. Hoshizaki, D. K., Hill, J. E. & Henry, S. A. The saccharomyces cerevisiae INO4 gene encodes a small, highly basic protein required for derepression of phospholipid biosynthetic enzymes. *J. Biol. Chem.* **265,** 4736–4745 (1990).

47. Robinson, K. A. & Lopes, J. M. The promoter of the yeast INO4 regulatory gene: A model of the simplest yeast promoter. *J. Bacteriol.* **182,** 2746–

2752 (2000).

48. Ashburner, B. P. & Lopes, J. M. Autoregulated expression of the yeast {INO2} and {INO4} helix-loop-helix activator genes effects cooperative regulation on their target genes. *Mol. Cell. Biol.* **15,** 1709–1715 (1995).

49. Henry, S. A., Kohlwein, S. D. & Carman, G. M. Metabolism and regulation of glycerolipids in the yeast Saccharomyces cerevisiae. *Genetics* **190,** 317–349 (2012).

50. Hasslacher, M., Ivessa, A. S., Paltauf, F. & Kohlwein, S. D. Acetyl-CoA carboxylase from yeast is an essential enzyme and is regulated by factors that control phospholipid metabolism. *J. Biol. Chem.* **268,** 10946–10952 (1993).

51. Grippa, A. *et al.* The seipin complex Fld1/Ldb16 stabilizes ER-lipid droplet contact sites. *J. Cell Biol.* **211,** 829–844 (2015).

52. Wolinski, H. *et al.* Seipin is involved in the regulation of phosphatidic acid metabolism at a subdomain of the nuclear envelope in yeast. *Biochim. Biophys. Acta - Mol. Cell Biol. Lipids* **1851,** 1450–1464 (2015).

53. Rajakumari, S., Rajasekharan, R. & Daum, G. Triacylglycerol lipolysis is linked to sphingolipid and phospholipid metabolism of the yeast Saccharomyces cerevisiae☆. *Biochim. Biophys. Acta - Mol. Cell Biol. Lipids*

1801, 1314–1322 (2010).

54. Athenstaedt, K. & Daum, G. Tgl4p and Tgl5p, two triacylglycerol lipases of the yeast Saccharomyces cerevisiae are localized to lipid particles. *J. Biol. Chem.* **280,** 37301–37309 (2005).

55. Lipid oxidation and autophagy in yeast. *Free Radic. Biol. Med.* **41,** 1655–1661 (2006).

56. Pu, J. *et al.* Interactomic study on interaction between lipid droplets and mitochondria. *Protein Cell* **2,** 487–496 (2011).

57. Athenstaedt, K. & Daum, G. YMR313c/TGL3 encodes a novel triacylglycerol lipase located in lipid particles of Saccharomyces cerevisiae. *J. Biol. Chem.* **278,** 23317–23 (2003).

58. Schmidt, C., Athenstaedt, K., Koch, B., Ploier, B. & Daum, G. Regulation of the yeast triacylglycerol lipase TGl3p by formation of nonpolar lipids. *J. Biol. Chem.* **288,** 19939–48 (2013).

59. Koch, B., Schmidt, C., Ploier, B. & Daum, G. Modifications of the C terminus affect functionality and stability of yeast triacylglycerol lipase Tgl3p. *J. Biol. Chem.* **289,** 19306–19316 (2014).

60. van Zutphen, T. *et al.* Lipid droplet autophagy in the yeast Saccharomyces cerevisiae. *Mol. Biol. Cell* **25,** 290–301 (2014).

61. Ploier, B. *et al.* Screening for hydrolytic enzymes reveals Ayr1p as a novel triacylglycerol lipase in Saccharomyces cerevisiae. *J. Biol. Chem.* **288,** 36061–72 (2013).

62. Rajakumari, S. & Daum, G. Multiple functions as lipase, steryl ester hydrolase, phospholipase, and acyltransferase of Tgl4p from the yeast Saccharomyces cerevisiae. *J. Biol. Chem.* **285,** 15769–76 (2010).

63. Klein, I. *et al.* Regulation of the yeast triacylglycerol lipases Tgl4p and Tgl5p by the presence/absence of nonpolar lipids. *Mol. Biol. Cell* **27,** 2014–2024 (2016).

64. Ham, H. J., Rho, H. J., Shin, S. K. & Yoon, H.-J. The TGL2 gene of Saccharomyces cerevisiae encodes an active acylglycerol lipase located in the mitochondria. *J. Biol. Chem.* **285,** 3005–13 (2010).

65. Athenstaedt, K. & Daum, G. 1-Acyldihydroxyacetone-phosphate reductase (Ayr1p) of the yeast Saccharomyces cerevisiae encoded by the open reading frame YIL124w is a major component of lipid particles. *J. Biol. Chem.* **275,** 235–240 (2000).

66. Zweytick, D. *et al.* Contribution of Are1p and Are2p to steryl ester synthesis in the yeast Saccharomyces cerevisiae. *Eur. J. Biochem.* **267,** 1075–82 (2000).

67. Athenstaedt, K., Zweytick, D., Jandrositz, A., Kohlwein, S. D. & Daum, G. Identification and characterization of major lipid particle proteins of the yeast Saccharomyces cerevisiae. *J. Bacteriol.* **181,** 6441–8 (1999).

68. Ploier, B. *et al.* Regulatory link between steryl ester formation and hydrolysis in the yeast Saccharomyces cerevisiae. *Biochim. Biophys. Acta - Mol. Cell Biol. Lipids* **1851,** 977–986 (2015).

69. Wagner, A., Grillitsch, K., Leitner, E. & Daum, G. Mobilization of steryl esters from lipid particles of the yeast Saccharomyces cerevisiae. *Biochim. Biophys. Acta - Mol. Cell Biol. Lipids* **1791,** 118–124 (2009).

70. Müllner, H., Deutsch, G., Leitner, E., Ingolic, E. & Daum, G. YEH2/YLR020c encodes a novel steryl ester hydrolase of the yeast Saccharomyces cerevisiae. *J. Biol. Chem.* **280,** 13321–13328 (2005).

71. Fei, W. *et al.* Genome-wide analysis of sterol-lipid storage and trafficking in Saccharomyces cerevisiae. *Eukaryot. Cell* **7,** 401–414 (2008).

72. Nguyen, T. B. *et al.* DGAT1-Dependent Lipid Droplet Biogenesis Protects Mitochondrial Function during Starvation-Induced Autophagy. *Dev. Cell* **42,** 9–21.e5 (2017).

73. Li, L. O., Klett, E. L. & Coleman, R. A. Acyl-CoA synthesis, lipid metabolism and lipotoxicity. *Biochim. Biophys. Acta - Mol. Cell Biol. Lipids* **1801,** 246–

251 (2010).

74. Richard, V. R. *et al.* Mechanism of liponecrosis, a distinct mode of programmed cell death. *Cell Cycle* **13,** 3707–26 (2014).

75. Sheibani, S. *et al.* Macromitophagy, neutral lipids synthesis, and peroxisomal fatty acid oxidation protect yeast from "liponecrosis", a previously unknown form of programmed cell death. *Cell Cycle* **13,** 138–47 (2014).

76. Wolinski, H. *et al.* Seipin is involved in the regulation of phosphatidic acid metabolism at a subdomain of the nuclear envelope in yeast. *Biochim. Biophys. Acta - Mol. Cell Biol. Lipids* **1851,** 1450–1464 (2015).

77. Poirier, Y., Antonenkov, V. D., Glumoff, T. & Hiltunen, J. K. Peroxisomal β-oxidation—A metabolic pathway with multiple functions. *Biochim. Biophys. Acta - Mol. Cell Res.* **1763,** 1413–1426 (2006).

78. Hiltunen, J. K. *et al.* The biochemistry of peroxisomal β-oxidation in the yeast *Saccharomyces cerevisiae*. *FEMS Microbiol. Rev.* **27,** 35–64 (2003).

79. Ouahoud, S. *et al.* Lipid droplet consumption is functionally coupled to vacuole homeostasis independent of lipophagy. *J. Cell Sci.* 1–15 (2018). doi:10.1242/jcs.213876

80. van Zutphen, T. *et al.* Lipid droplet autophagy in the yeast Saccharomyces

cerevisiae. *Mol. Biol. Cell* **25,** 290–301 (2014).

81. Fatty Acid Trafficking in Starved Cells: Regulation by Lipid Droplet Lipolysis, Autophagy, and Mitochondrial Fusion Dynamics. *Dev. Cell* **32,** 678–692 (2015).

82. Rambold, A. S., Cohen, S. & Lippincott-Schwartz, J. Fatty acid trafficking in starved cells: Regulation by lipid droplet lipolysis, autophagy, and mitochondrial fusion dynamics. *Dev. Cell* **32,** 678–692 (2015).

83. Skinner, J. R. *et al.* Diacylglycerol enrichment of endoplasmic reticulum or lipid droplets recruits perilipin 3/TIP47 during lipid storage and mobilization. *J. Biol. Chem.* **284,** 30941–30948 (2009).

84. Orlean, P. Architecture and biosynthesis of the Saccharomyces cerevisiae cell wall. *Genetics* **192,** 775–818 (2012).

85. Lesage, G. & Bussey, H. Cell wall assembly in Saccharomyces cerevisiae. *Microbiol. Mol. Biol. Rev.* **70,** 317–43 (2006).

86. de Groot, P. W. J., Hellingwerf, K. J. & Klis, F. M. Genome-wide identification of fungal GPI proteins. *Yeast* (2003). doi:10.1002/yea.1007

87. Subramanya, S., Hardin, C. F., Steverding, D. & Mensa-Wilmot, K. Glycosylphosphatidylinositol-specific phospholipase C regulates transferrin endocytosis in the African trypanosome. *Biochem. J.* **417,**

685–694 (2009).

88. Levin, D. E. Cell Wall Integrity Signaling in Saccharomyces cerevisiae Cell. *Microbiol Mol Biol Rev* (2005). doi:10.1128/MMBR.69.2.262

89. Kono, K. *et al.* G1/S Cyclin-dependent Kinase Regulates Small GTPase Rho1p through Phosphorylation of RhoGEF Tus1p in *Saccharomyces cerevisiae*. *Mol. Biol. Cell* **19,** 1763–1771 (2008).

90. Davenport, K. R., Sohaskey, M., Kamada, Y., Levin, D. E. & Gustin, M. C. A second osmosensing signal transduction pathway in yeast. Hypotonic shock activates the PKC1 protein kinase-regulated cell integrity pathway. *J. Biol. Chem.* **270,** 30157–61 (1995).

91. Levin, D. E. Cell wall integrity signaling in Saccharomyces cerevisiae. *Microbiol. Mol. Biol. Rev.* **69,** 262–91 (2005).

92. Robciuc, A., Hyötyläinen, T., Jauhiainen, M. & Holopainen, J. M. Hyperosmolarity-induced lipid droplet formation depends on ceramide production by neutral sphingomyelinase 2. *J. Lipid Res.* **53,** 2286–2295 (2012).

93. Kamada, Y., Jung, U. S., Piotrowski, J. & Levin, D. E. The protein kinase C-activated MAP kinase pathway of Saccharomyces cerevisiae mediates a novel aspect of the heat shock response. *Genes Dev.* **9,** 1559–71 (1995).

94. Park, J. I., Collinson, E. J., Grant, C. M. & Dawes, I. W. Rom2p, the Rho1 GTP/GDP exchange factor of Saccharomyces cerevisiae, can mediate stress responses via the Ras-cAMP pathway. *J. Biol. Chem.* (2005). doi:10.1074/jbc.M407900200

95. Philip, B. & Levin, D. E. Wsc1 and Mid2 Are Cell Surface Sensors for Cell Wall Integrity Signaling That Act through Rom2, a Guanine Nucleotide Exchange Factor for Rho1. *Mol. Cell. Biol.* (2001). doi:10.1128/MCB.21.1.271-280.2001

96. Delley, P. A. & Hall, M. N. Cell wall stress depolarizes cell growth via hyperactivation of RHO1. *J. Cell Biol.* (1999). doi:10.1083/jcb.147.1.163

97. Magie, C. R., Meyer, M. R., Gorsuch, M. S. & Parkhurst, S. M. Mutations in the Rho1 small GTPase disrupt morphogenesis and segmentation during early Drosophila development. *Development* (1999).

98. Guo, S. *et al.* A MAP kinase dependent feedback mechanism controls Rho1 GTPase and actin distribution in yeast. *PLoS One* (2009). doi:10.1371/journal.pone.0006089

99. Schmelzle, T., Helliwell, S. B. & Hall, M. N. Yeast protein kinases and the RHO1 exchange factor TUS1 are novel components of the cell integrity pathway in yeast. *Mol. Cell. Biol.* **22,** 1329–39 (2002).

100. Krause, S. A. *et al.* Functional specialisation of yeast Rho1 GTP exchange factors. *J. Cell Sci.* (2012). doi:10.1242/jcs.100685

101. Serrano, R., Martín, H., Casamayor, A. & Ariño, J. Signaling alkaline pH stress in the yeast Saccharomyces cerevisiae through the Wsc1 cell surface sensor and the Slt2 MAPK pathway. *J. Biol. Chem.* (2006). doi:10.1074/jbc.M604497200

102. Martín, H., Rodríguez-Pachón, J. M., Ruiz, C., Nombela, C. & Molina, M. Regulatory mechanisms for modulation of signaling through the cell integrity Slt2-mediated pathway in Saccharomyces cerevisiae. *J. Biol. Chem.* **275,** 1511–9 (2000).

103. Raucher, D. *et al.* Phosphatidylinositol 4,5-bisphosphate functions as a second messenger that regulates cytoskeleton-plasma membrane adhesion. *Cell* (2000). doi:10.1016/S0092-8674(00)81560-3

104. Audhya, A. & Emr, S. D. Stt4 PI 4-kinase localizes to the plasma membrane and functions in the Pkc1-mediated MAP kinase cascade. *Dev. Cell* **2,** 593–605 (2002).

105. Helliwell, S. B., Schmidt, A., Ohya, Y. & Hall, M. N. The Rho1 effector Pkc1, but not Bni1, mediates signalling from Tor2 to the actin cytoskeleton. *Curr. Biol.* (1998). doi:10.1016/S0960-9822(07)00511-8

106. Kamada, Y. *et al.* Activation of yeast protein kinase C by Rho1 GTPase. *J. Biol. Chem.* (1996). doi:10.1074/jbc.271.16.9193

107. Rodríguez-Peña, J. M., Díez-Muñiz, S., Bermejo, C., Nombela, C. & Arroyo, J. Activation of the yeast cell wall integrity MAPK pathway by zymolyase depends on protease and glucanase activities and requires the mucin-like protein Hkr1 but not Msb2. *FEBS Lett.* (2013). doi:10.1016/j.febslet.2013.09.030

108. Bermejo, C. *et al.* The Sequential Activation of the Yeast HOG and SLT2 Pathways Is Required for Cell Survival to Cell Wall Stress. *Mol. Biol. Cell* **19,** 1113–1124 (2008).

109. Kim, K.-Y., Truman, A. W. & Levin, D. E. Yeast Mpk1 Mitogen-Activated Protein Kinase Activates Transcription through Swi4/Swi6 by a Noncatalytic Mechanism That Requires Upstream Signal. *Mol. Cell. Biol.* (2008). doi:10.1128/MCB.01795-07

110. Gray, J. V. *et al.* A role for the Pkc1 MAP kinase pathway of Saccharomyces cerevisiae in bud emergence and identification of a putative upstream regulator. *EMBO J.* (1997). doi:10.1093/emboj/16.16.4924

111. Roncero, C. & Durán, A. Effect of Calcofluor white and Congo red on

fungal cell wall morphogenesis: in vivo activation of chitin polymerization. *J. Bacteriol.* **163,** 1180–5 (1985).

112. Levin, D. E. Regulation of cell wall biogenesis in Saccharomyces cerevisiae: The cell wall integrity signaling pathway. *Genetics* (2011). doi:10.1534/genetics.111.128264

113. Csordás, G. *et al.* Structural and functional features and significance of the physical linkage between ER and mitochondria. *J. Cell Biol.* **174,** 915–921 (2006).

114. Lahiri, S. *et al.* A Conserved Endoplasmic Reticulum Membrane Protein Complex (EMC) Facilitates Phospholipid Transfer from the ER to Mitochondria. *PLoS Biol.* **12,** (2014).

115. Shiao, Y. J., Lupo, G. & Vance, J. E. Evidence that phosphatidylserine is imported into mitochondria via a mitochondria-associated membrane and that the majority of mitochondrial phosphatidylethanolamine is derived from decarboxylation of phosphatidylserine. *J. Biol. Chem.* **270,** 11190–11198 (1995).

116. Achleitner, G. *et al.* Association between the endoplasmic reticulum and mitochondria of yeast facilitates interorganelle transport of phospholipids through membrane contact. *Eur. J. Biochem.* **264,** 545–553

(1999).

117. Murley, A. *et al.* ER-associated mitochondrial division links the distribution of mitochondria and mitochondrial DNA in yeast. *Elife* **2013,** 1–16 (2013).

118. Lang, A., John Peter, A. T. & Kornmann, B. ER-mitochondria contact sites in yeast: Beyond the myths of ERMES. *Curr. Opin. Cell Biol.* **35,** 7–12 (2015).

119. Murley, A. *et al.* Ltc1 is an ER-localized sterol transporter and a component of ER-mitochondria and ER-vacuole contacts. *J. Cell Biol.* **209,** 539–548 (2015).

120. Böckler, S. & Westermann, B. Mitochondrial ER contacts are crucial for mitophagy in yeast. *Dev. Cell* **28,** 450–458 (2014).

121. Kannan, M., Sivaprakasam, C., Prinz, W. A. & Nachiappan, V. Endoplasmic reticulum stress affects the transport of phosphatidylethanolamine from mitochondria to the endoplasmic reticulum in S. cerevisiae. *Biochim. Biophys. Acta - Mol. Cell Biol. Lipids* **1861,** 1959–1967 (2016).

122. Gaigg, B., Simbeni, R., Hrastnik, C., Paltauf, F. & Daum, G. Characterization of a microsomal subfraction associated with. **1234,** 214–220 (1995).

123. Tamura, Y. *et al.* Phosphatidylethanolamine biosynthesis in mitochondria: Phosphatidylserine (PS) trafficking is independent of a PS decarboxylase and intermembrane space proteins Ups1p and Ups2p. *J. Biol. Chem.* **287,** 43961–43971 (2012).

124. Nebauer, R., Schuiki, I., Kulterer, B., Trajanoski, Z. & Daum, G. The phosphatidylethanolamine level of yeast mitochondria is affected by the mitochondrial components Oxa1p and Yme1p. *FEBS J.* **274,** 6180–6190 (2007).

125. ER fatalities—The role of ER-mitochondrial contact sites in yeast life and death decisions. *Mech. Ageing Dev.* **161,** 225–233 (2017).

126. Voss, C., Lahiri, S., Young, B. P., Loewen, C. J. & Prinz, W. A. ER-shaping proteins facilitate lipid exchange between the ER and mitochondria in S. cerevisiae. *J. Cell Sci.* **125,** 4791–4799 (2012).

127. Becker, T. *et al.* Role of phosphatidylethanolamine in the biogenesis of mitochondrial outer membrane proteins. *J. Biol. Chem.* **288,** 16451–16459 (2013).

128. Dimmer, K. S. & Rapaport, D. Mitochondrial contact sites as platforms for phospholipid exchange. *Biochim. Biophys. Acta - Mol. Cell Biol. Lipids* **1862,** 69–80 (2017).

129. Rowland, A. A. & Voeltz, G. K. Endoplasmic reticulum–mitochondria contacts: function of the junction. *Nat. Rev. Mol. Cell Biol.* **13,** 607–625 (2012).

130. Gsell, M. *et al.* Transcriptional Response to Deletion of the Phosphatidylserine Decarboxylase Psd1p in the Yeast Saccharomyces cerevisiae. *PLoS One* **8,** (2013).

131. Horvath, S. E. *et al.* Processing and topology of the yeast mitochondrial phosphatidylserine decarboxylase. *J. Biol. Chem.* **287,** 36744–36755 (2012).

132. Zaremberg, V. & McMaster, C. R. Differential partitioning of lipids metabolized by separate yeast glycerol-3-phosphate acyltransferases reveals that phospholipase D generation of phosphatidic acid mediates sensitivity to choline-containing lysolipids and drugs. *J. Biol. Chem.* **277,** 39035–39044 (2002).

133. Aaltonen, M. J. *et al.* MICOS and phospholipid transfer by Ups2-Mdm35 organize membrane lipid synthesis in mitochondria. *J. Cell Biol.* **213,** 525–34 (2016).

134. Weisshaar, N., Welsch, H., Guerra-Moreno, A. & Hanna, J. Phospholipase Lpl1 links lipid droplet function with quality control protein degradation.

Mol. Biol. Cell **28,** 716–725 (2017).

135. Jiang, F. *et al.* Absence of cardiolipin in the crd1 null mutant results in decreased mitochondrial membrane potential and reduced mitochondrial function. *J. Biol. Chem.* **275,** 22387–22394 (2000).

136. Su, X. & Dowhan, W. Regulation of cardiolipin synthase levels in Saccharomyces cerevisiae. *Yeast* **23,** 279–291 (2006).

137. Joshi, A. S., Thompson, M. N., Fei, N., Ttemann, M. H. & Greenberg, M. L. Cardiolipin and mitochondrial phosphatidylethanolamine have overlapping functions in mitochondrial fusion in Saccharomyces cerevisiae. *J. Biol. Chem.* **287,** 17589–17597 (2012).

138. Birk, A. V., Chao, W. M., Bracken, C., Warren, J. D. & Szeto, H. H. Targeting mitochondrial cardiolipin and the cytochrome c/cardiolipin complex to promote electron transport and optimize mitochondrial ATP synthesis. *Br. J. Pharmacol.* **171,** 2017–2028 (2014).

139. Robinson, N. C. Functional binding of cardiolipin to cytochrome c oxidase. *J. Bioenerg. Biomembr.* **25,** 153–163 (1993).

140. Goldberg, A. A. *et al.* A novel function of lipid droplets in regulating longevity. *Biochem. Soc. Trans.* **37,** 1050–5 (2009).

141. Welte, M. A. Proteins under new management: lipid droplets deliver.

Trends Cell Biol. **17,** 363–369 (2007).

142. Gueldener, U., Heinisch, J., Koehler, G. J., Voss, D. & Hegemann, J. H. A second set of loxP marker cassettes for Cre-mediated multiple gene knockouts in budding yeast. *Nucleic Acids Res.* **30,** e23 (2002).

143. Lappalainen, P., Fedorov, E. V, Fedorov, A. A., Almo, S. C. & Drubin, D. G. Essential functions and actin-binding surfaces of yeast cofilin revealed by systematic mutagenesis. *EMBO J.* **16,** 5520–30 (1997).

144. Arrese, E. L., Saudale, F. Z. & Soulages, J. L. Lipid Droplets as Signaling Platforms Linking Metabolic and Cellular Functions. *Lipid Insights* **7,** 7–16 (2014).

145. Kwolek-Mirek, M. & Zadrag-Tecza, R. Comparison of methods used for assessing the viability and vitality of yeast cells. *FEMS Yeast Res.* **14,** n/a-n/a (2014).

146. Carmona-Gutierrez, D. *et al.* Guidelines and recommendations on yeast cell death nomenclature. *Microb. cell (Graz, Austria)* **5,** 4–31 (2018).

147. Miner, G. E., Starr, M. L., Hurst, L. R. & Fratti, R. A. Deleting the DAG kinase Dgk1 augments yeast vacuole fusion through increased Ypt7 activity and altered membrane fluidity. *Traffic* **18,** 315–329 (2017).

148. Yonezawa, N., Nishidas, E., Iidaq, K., Yaharag, I. & Sakai, H. *Inhibition of*

*the Interactions of Cofilin, Destrin, and Deoxyribonuclease I with Actin by Phosphoinositides**. *THE JOURNAL OF BIOLOGICAL CHEM~~Y* **8,**

149. Zhao, H., Hakala, M. & Lappalainen, P. ADF/cofilin binds phosphoinositides in a multivalent manner to act as a PIP(2)-density sensor. *Biophys. J.* **98,** 2327–36 (2010).

150. Pauli J. Ojala, Ville Paavilainen, and & Lappalainen*, P. Identification of Yeast Cofilin Residues Specific for Actin Monomer and PIP2 Binding†. (2001). doi:10.1021/BI0117697